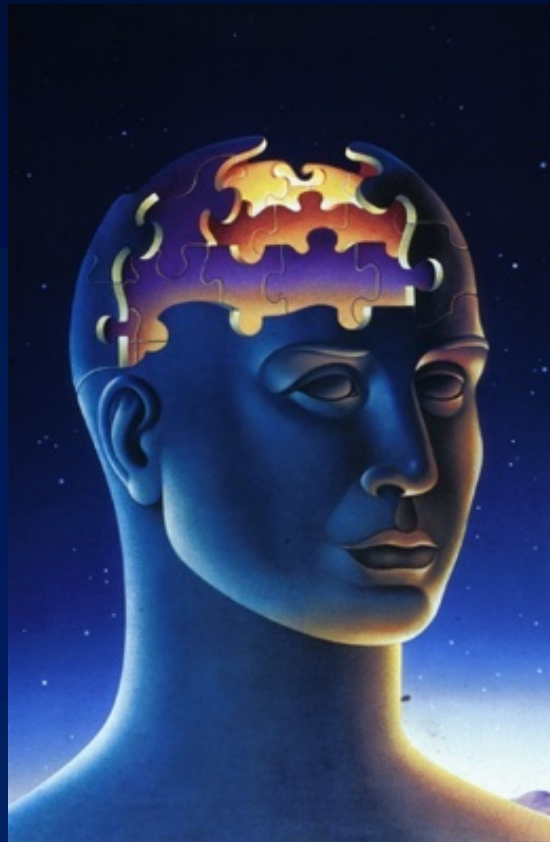
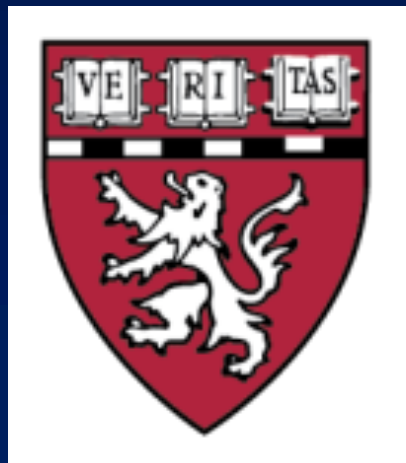


Cortical Circuits

1. Example from Epilepsy 2. General Principles

Stelios M Smirnakis

Brigham and Women's H., JP VA, Harvard Medical School



Collaborators,

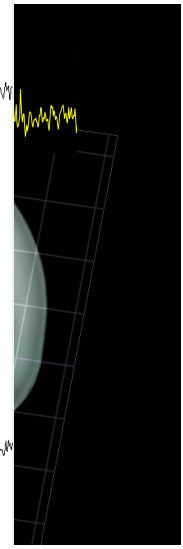
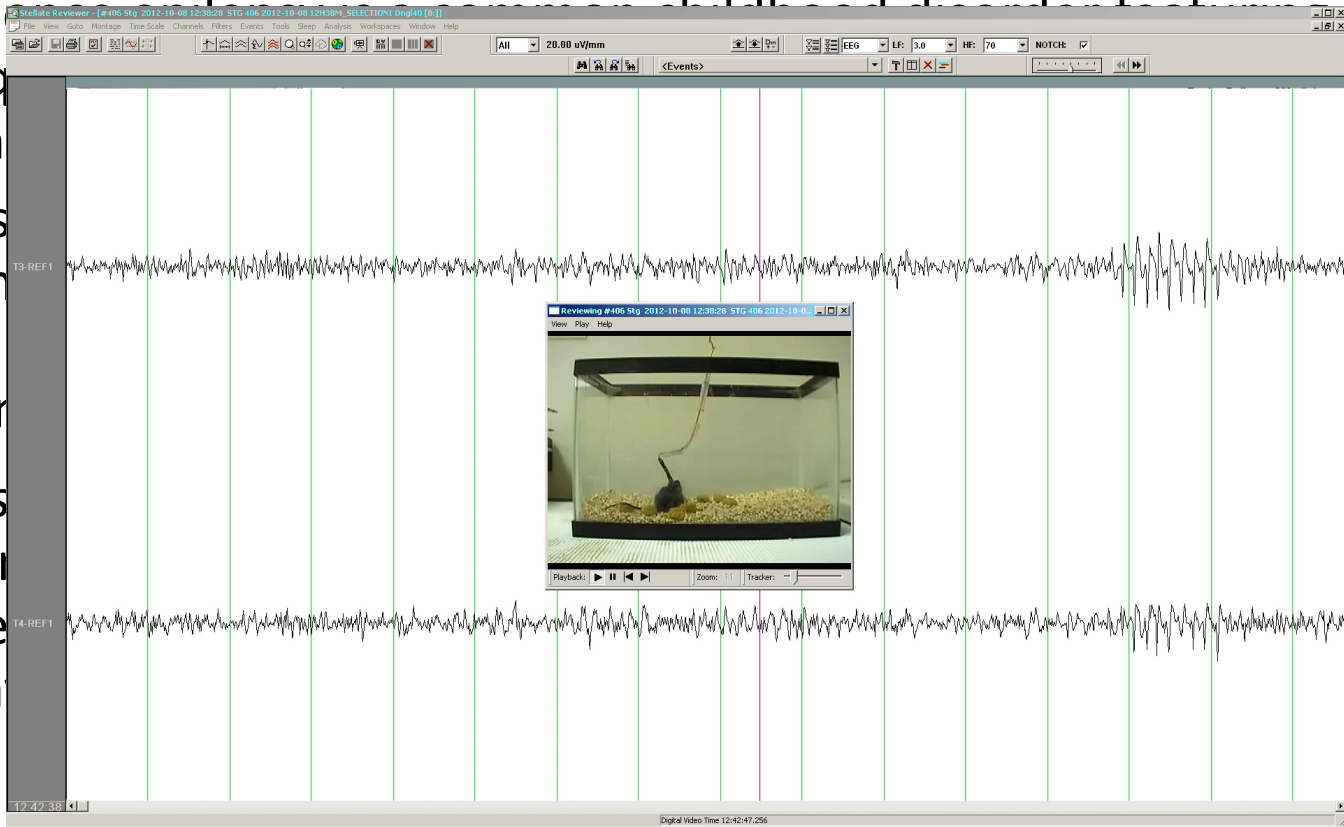
- Atul Maheshwari
- Jochen Meyer
- Jeffrey Noebels
- Xiaolong Jiang

Baylor
College of
Medicine

Example from Epilepsy Analysis

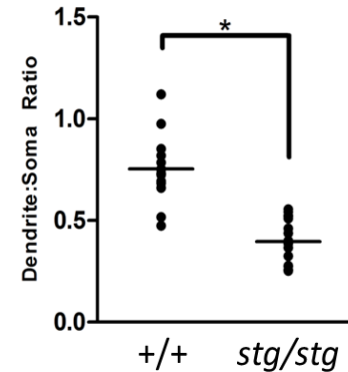
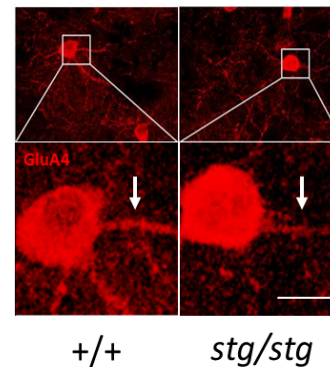
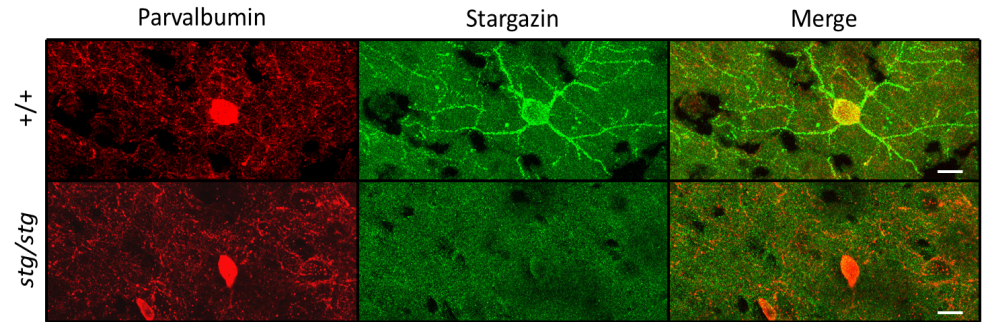
- None

- Absence of high frequency behavior
- The subject often hyperactive and more active
- The subject absent wave behavior

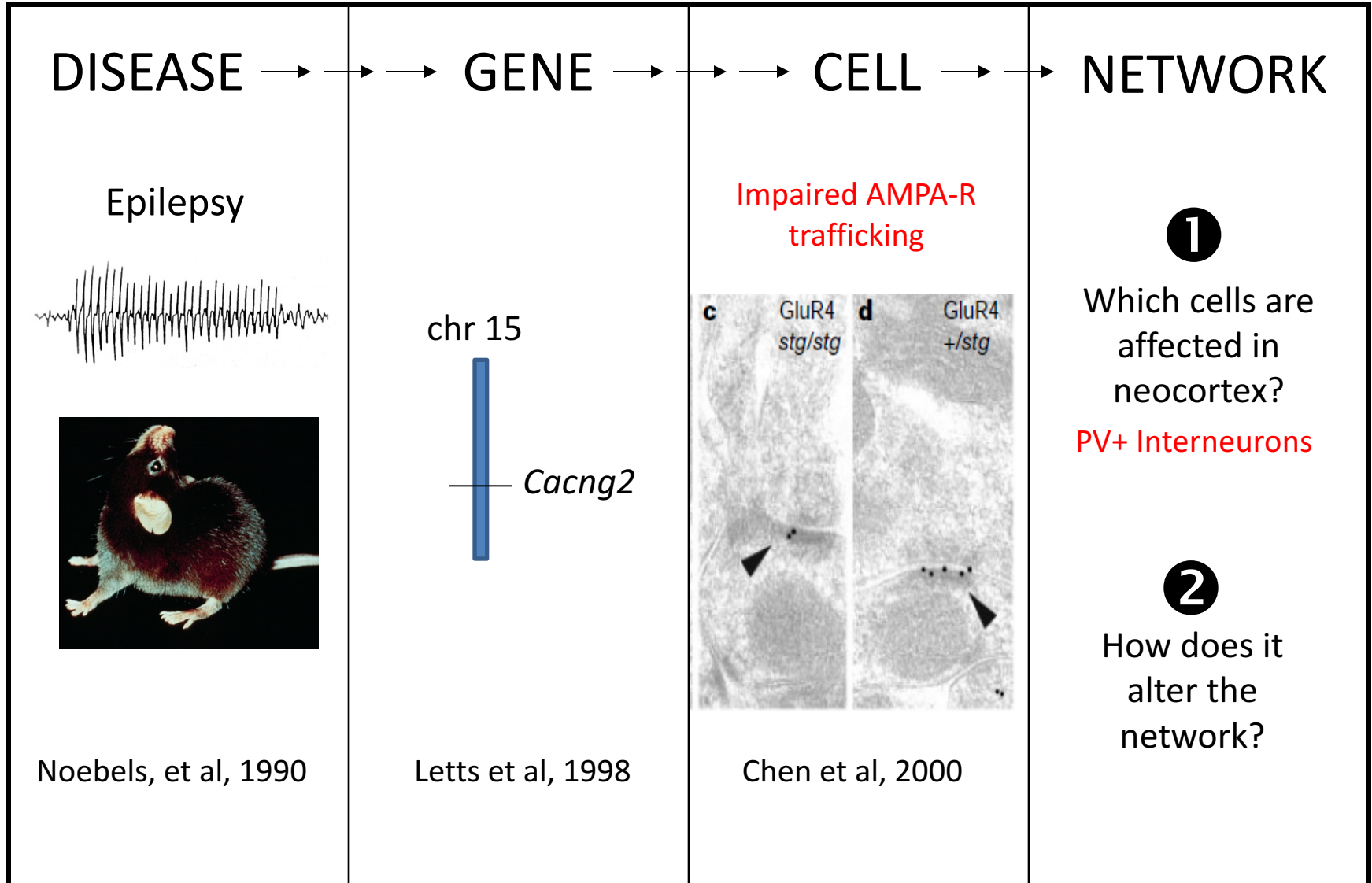


- The mutation in *stargazer* mice leads to loss of the TARP subunit *CACNG2*, which results in mis-trafficking of dendritic AMPA receptors in fast-spiking interneurons in the neocortex and thalamus.

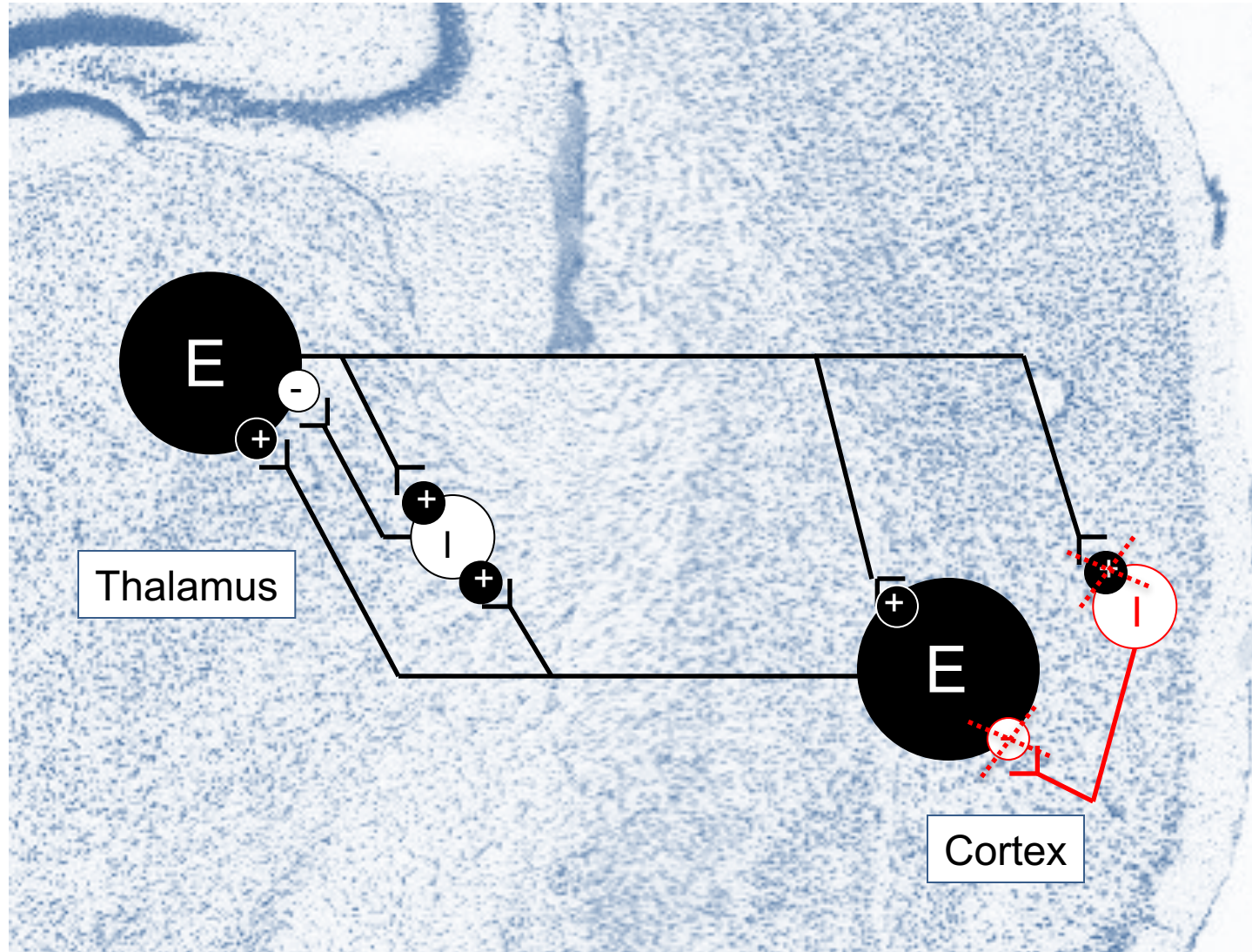
Stargazin: PV-specific cortical expression



Stargazer: From Disease to Target

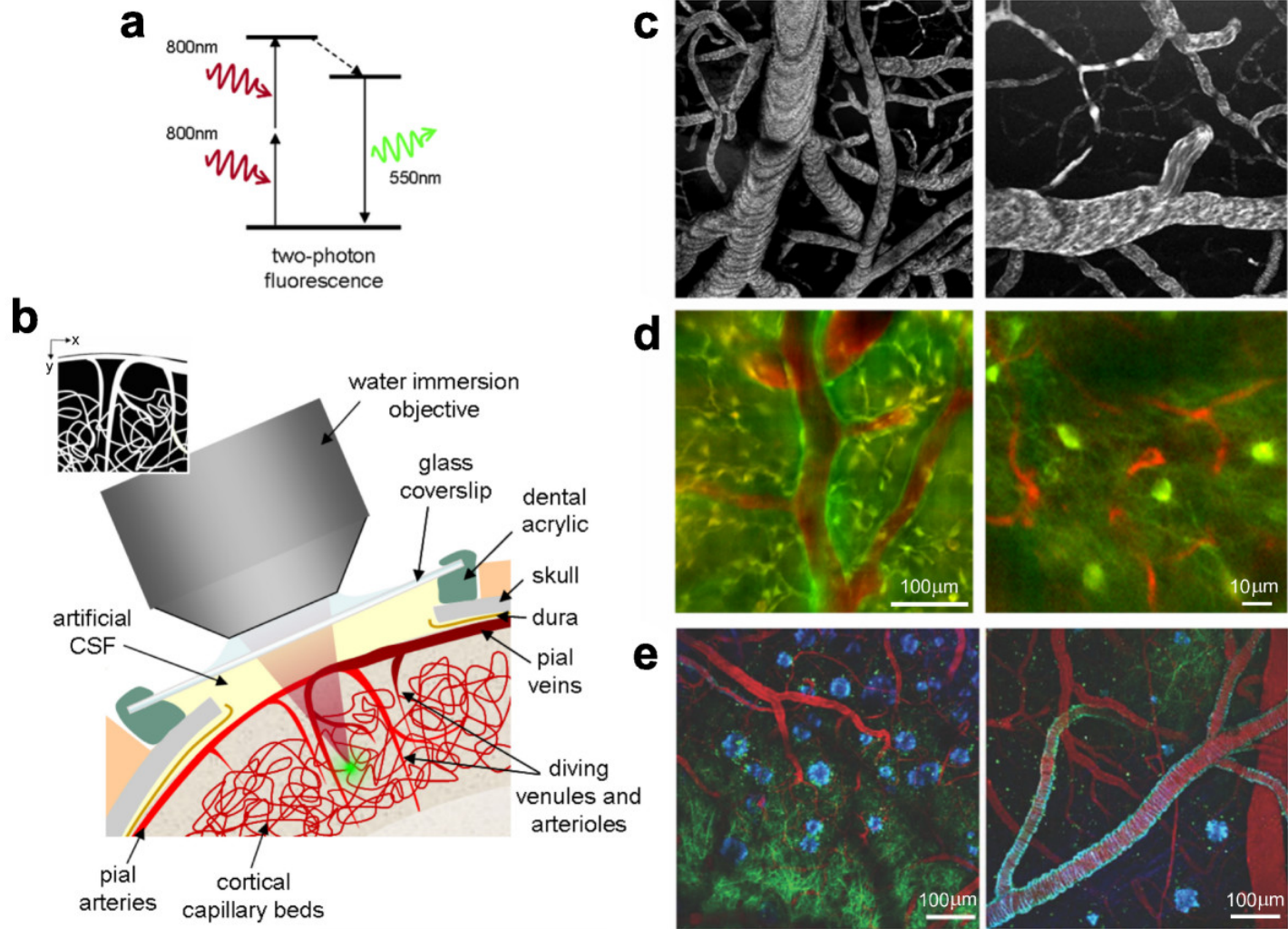


Absence Seizure Network



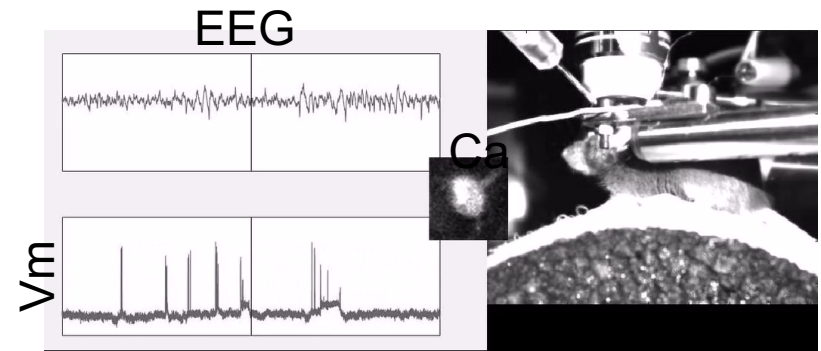
However this has not been tested in vivo in the functioning cortical circuit at cellular resolution

In vivo 2-photon microscopy



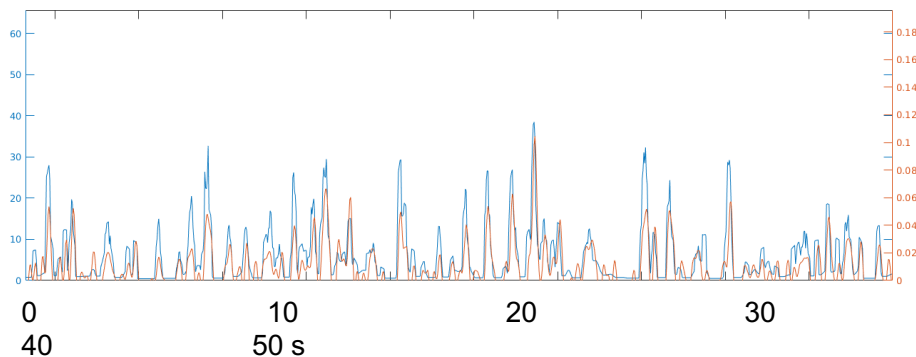
In vivo two-photon microscopy

- The calcium signal is a well-established surrogate measure of electrical activity in neurons.
- We recorded neuron and neuropil activity profiles chronically, in awake stg/stg mice, using GCamp6, while simultaneously recording EEG.

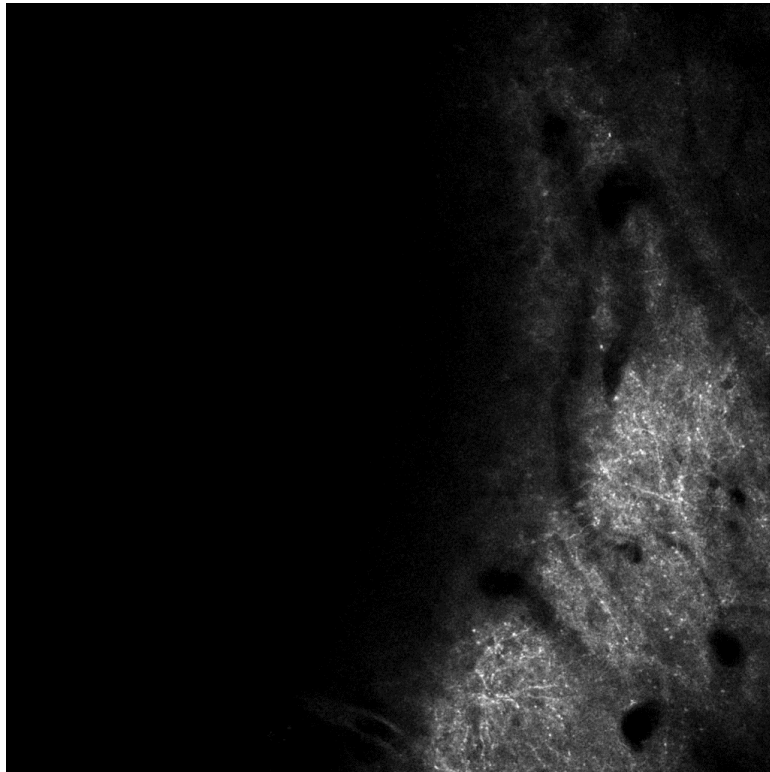


Gcamp6-patch validation

L2/3 pyr stg/stg; *blue*: e-phys, *orange*: dF/F

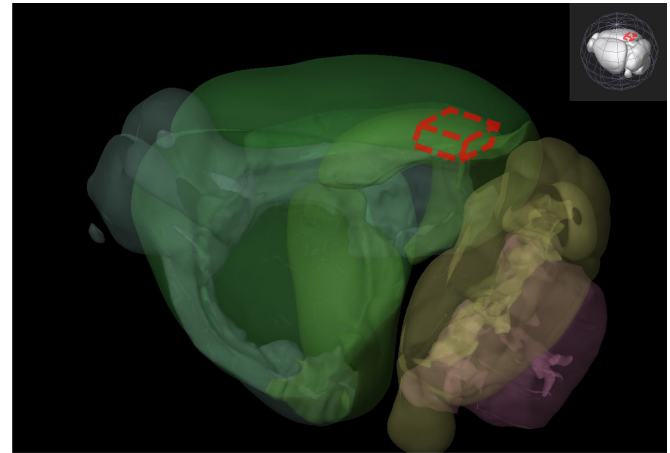


3 mm craniotomy over V1

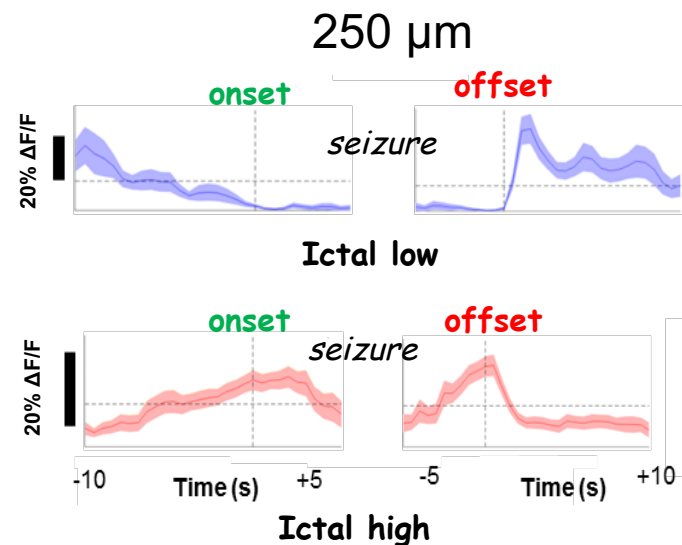
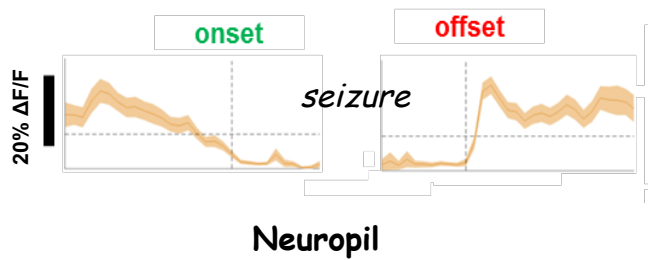
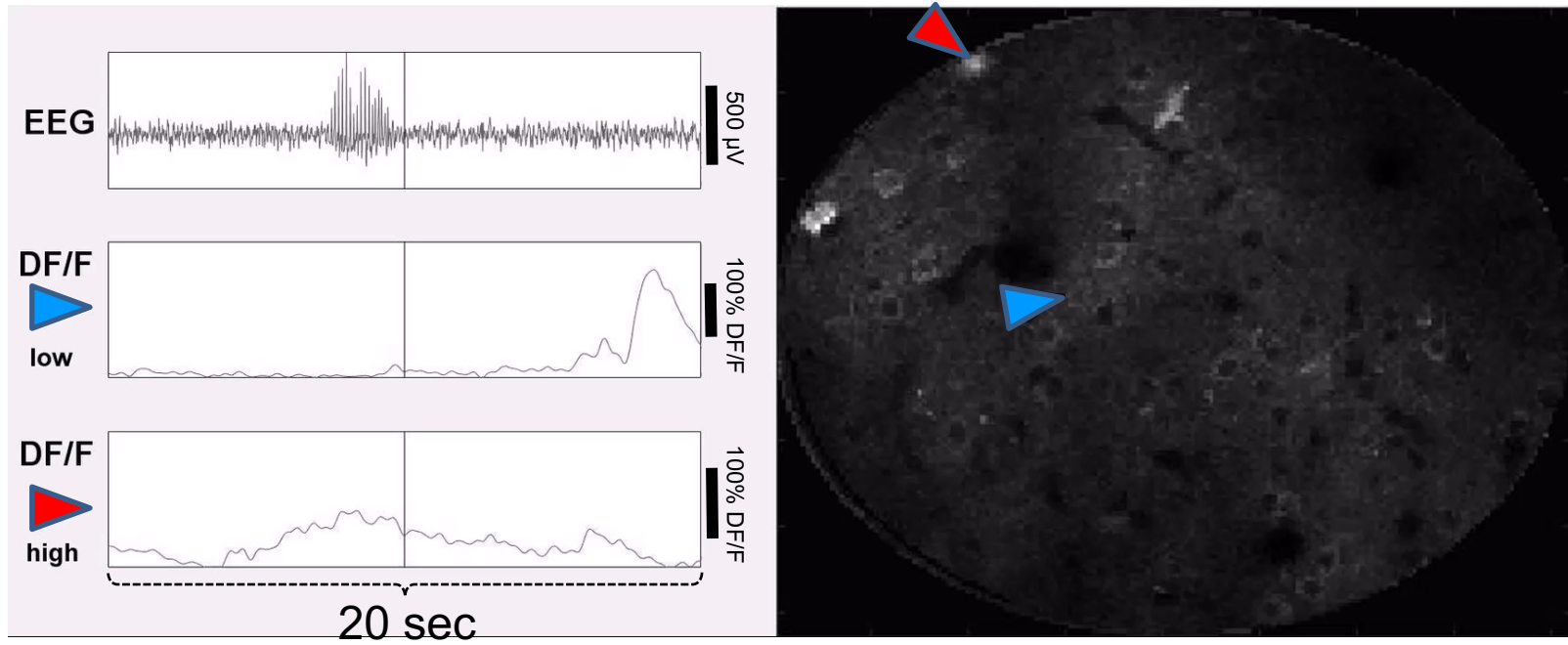


800 μm

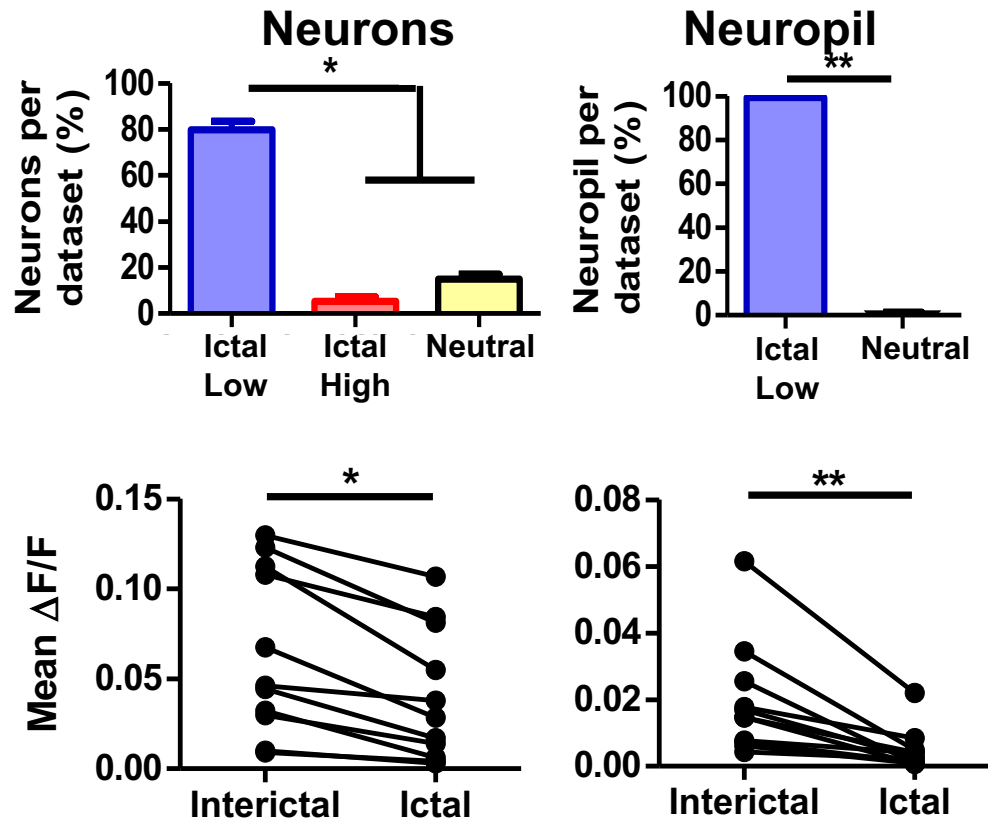
Approximate location of z-stack



Example of simultaneous EEG and calcium imaging

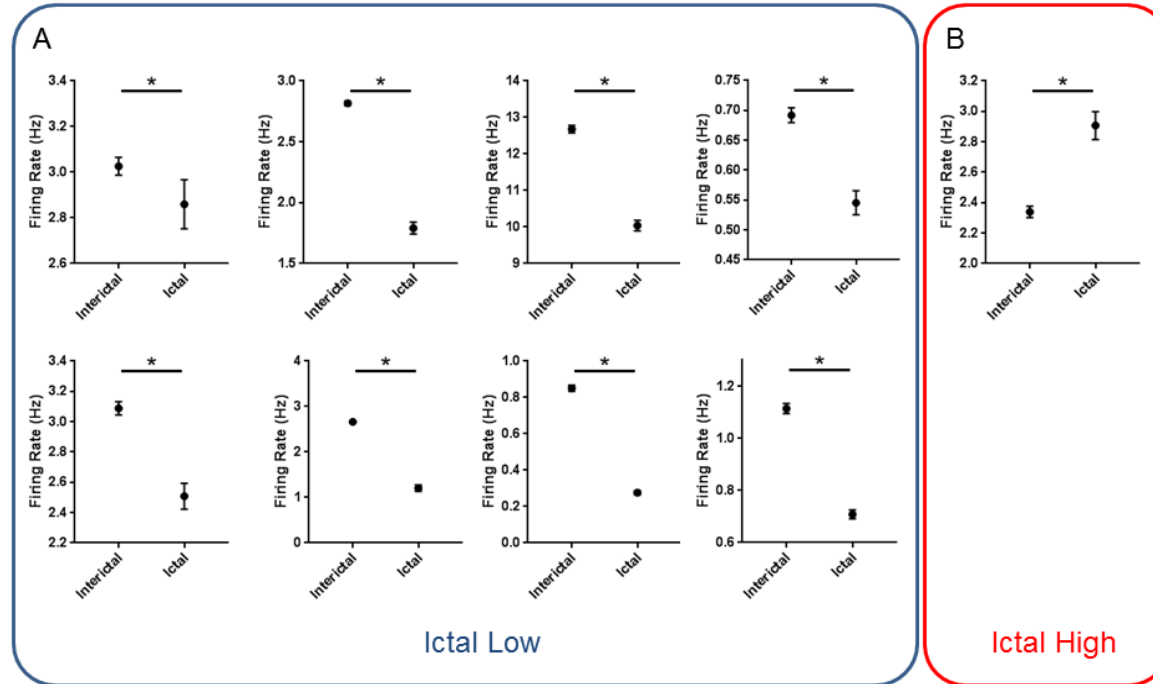


The majority of neuronal and neuropil activity is significantly suppressed during seizures in mouse V1 L2/3



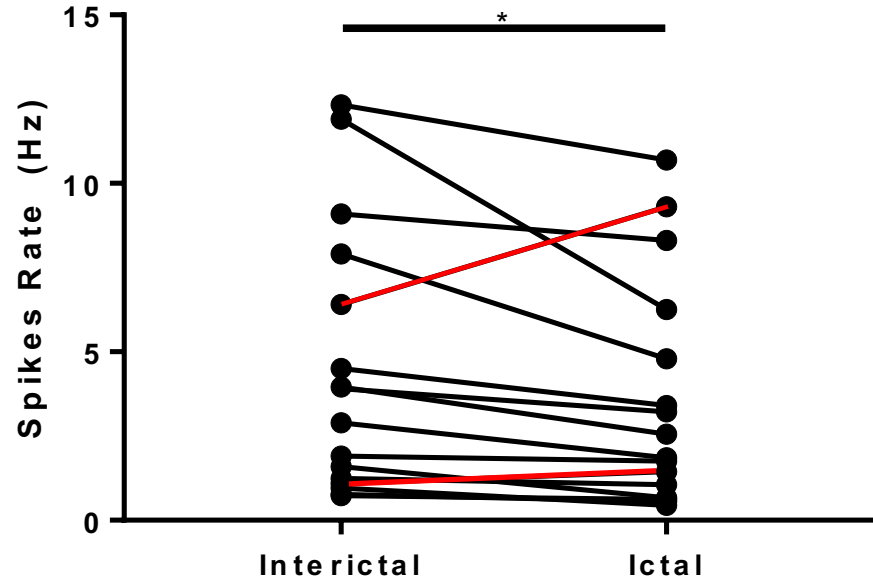
Asynchronous suppression of visual cortex during absence seizures
Jochen Meyer¹, Atul Maheshwari¹, Jeffrey Noebels* and Stelios Smirnakis**
(Nat Comm, under review)

Patch-clamp recordings in a subset of animals corroborate the predominant ictal-low character of L2/3 neurons



Mean \pm SEM ictal and interictal firing rates calculated from action potentials. 8 of 9 cells were deemed ictal low (A), whereas 1 cell was ictal high (B); * $p < 0.005$, Mann-Whitney U test.

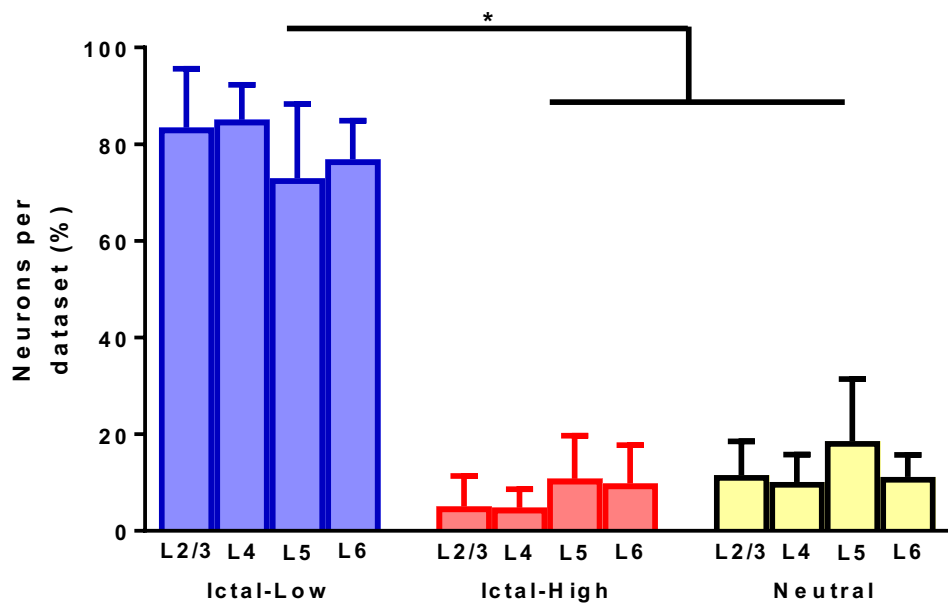
Patched Pyramidal Neuron summary



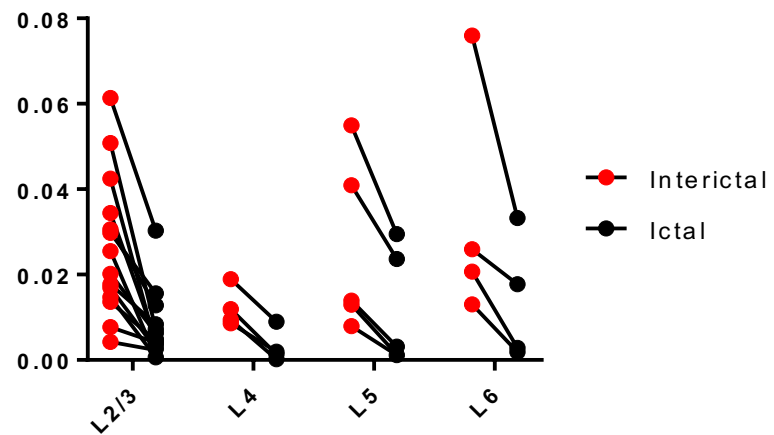
- 15 ictal lows, 2 ictal highs
- Wilcoxon paired rank-sum $p=0.0092$

Is this specific for L2/3?

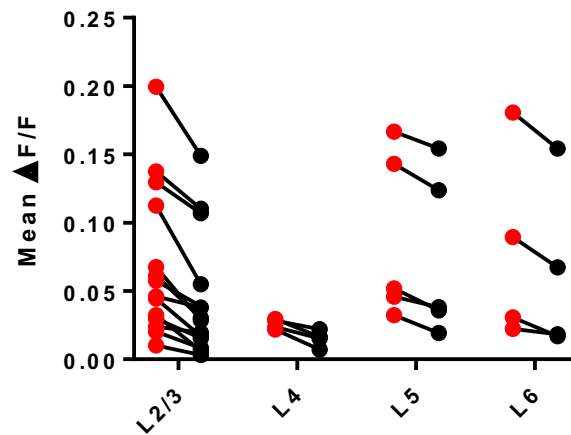
Neurons by both class and layer



Neuropil

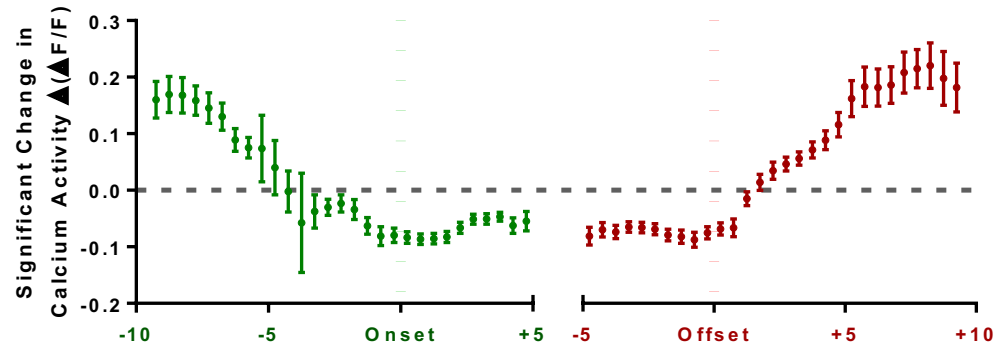


Neurons

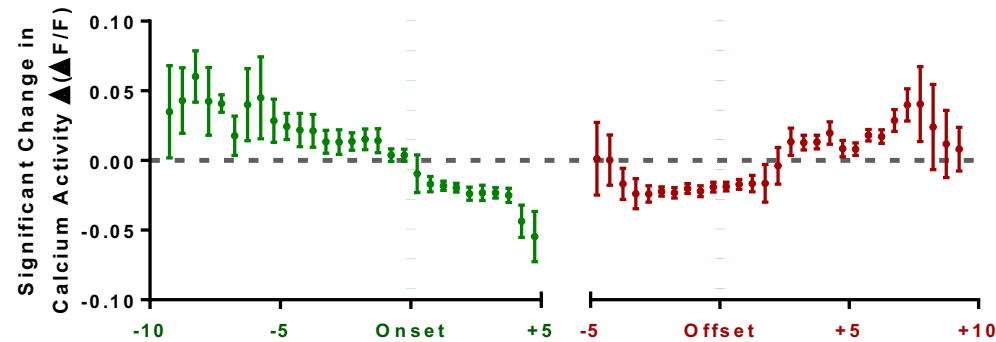


Ictal Low Neuron Seizure Participation

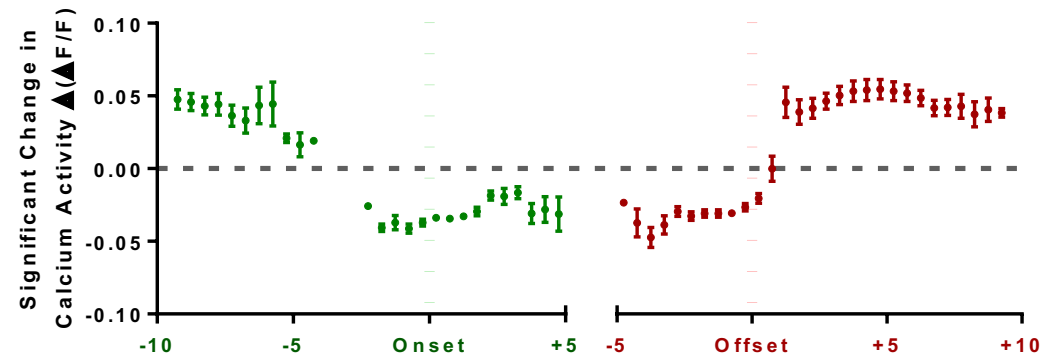
Layer 2/3



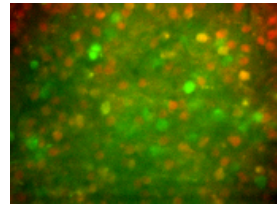
Layer 5



Layer 6



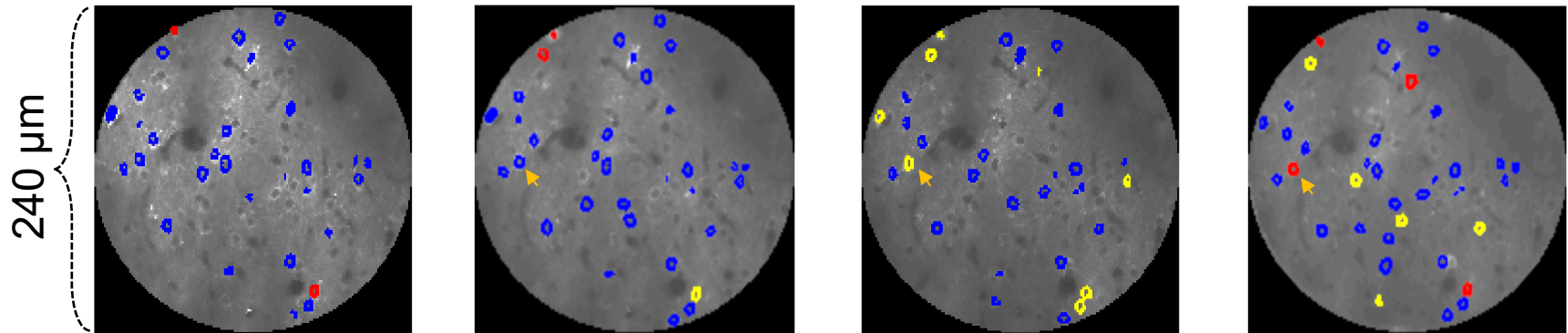
NOCOR-Cre x Ai9
stg/stg



730 μ m below dura

Temporal coupling with seizures is loose, spatial arrangements change over time.

The same group of neurons imaged chronically over 8 consecutive days



Day 1, 1st recording

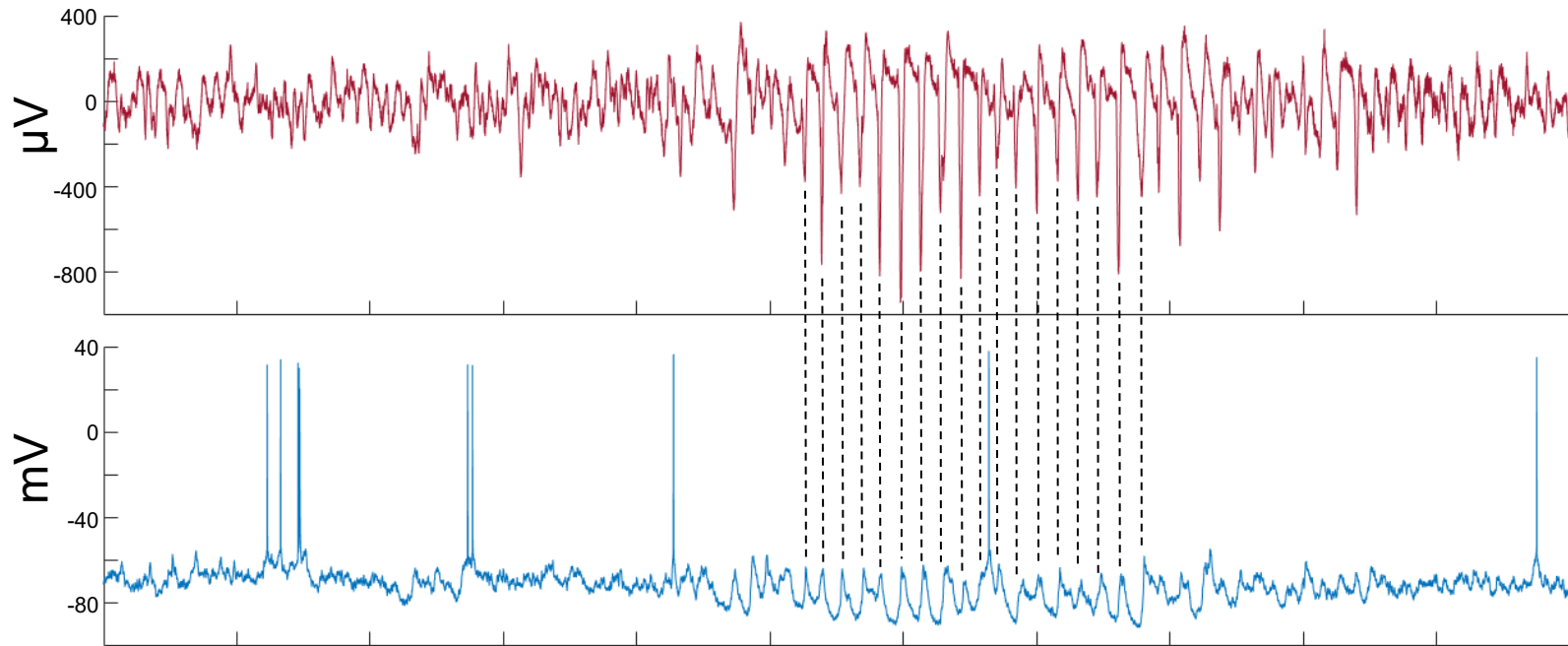
Day 1, 2nd recording

Day 4

Day 8

- = ictal high neuron
- = ictal low neuron
- = neutral neuron

Subthreshold oscillations can coincide with seizures

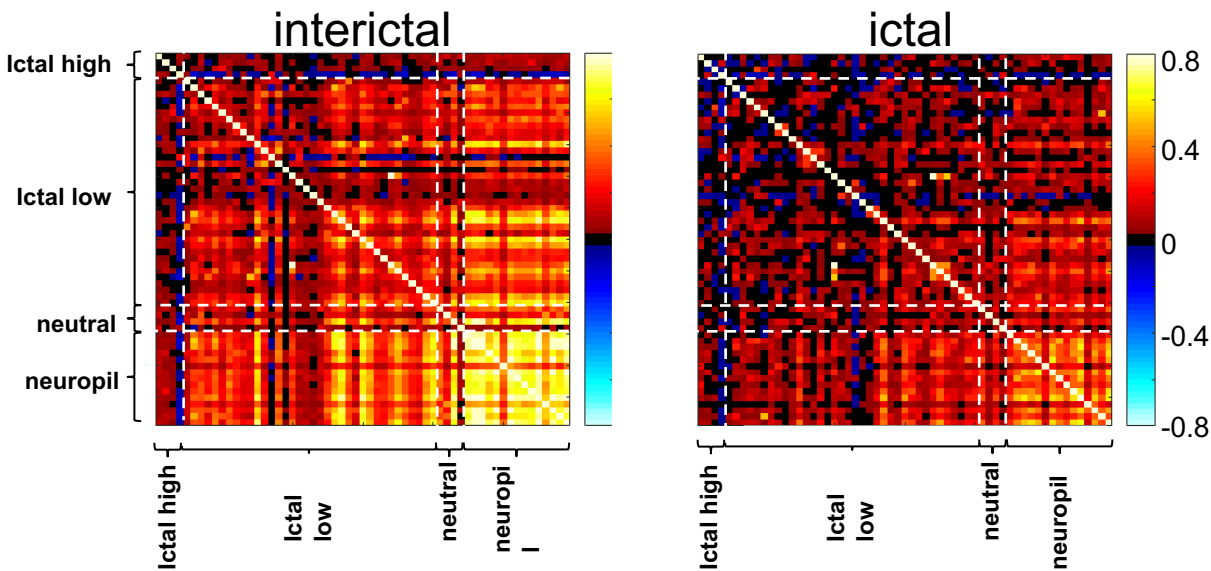


However neuronal engagement to seizures is flexible

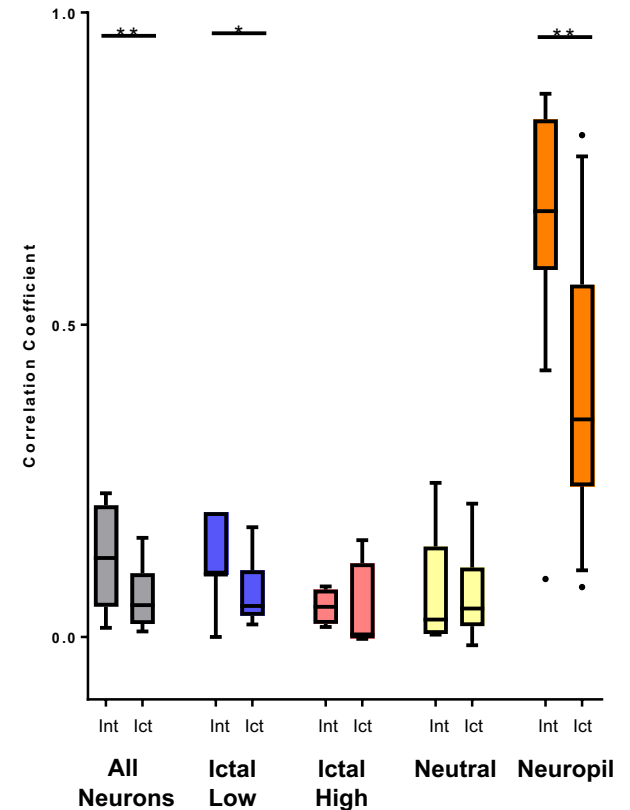
What happens to synchrony?

Pair-wise synchrony drops significantly during seizures, in both neurons and neuropil patches.

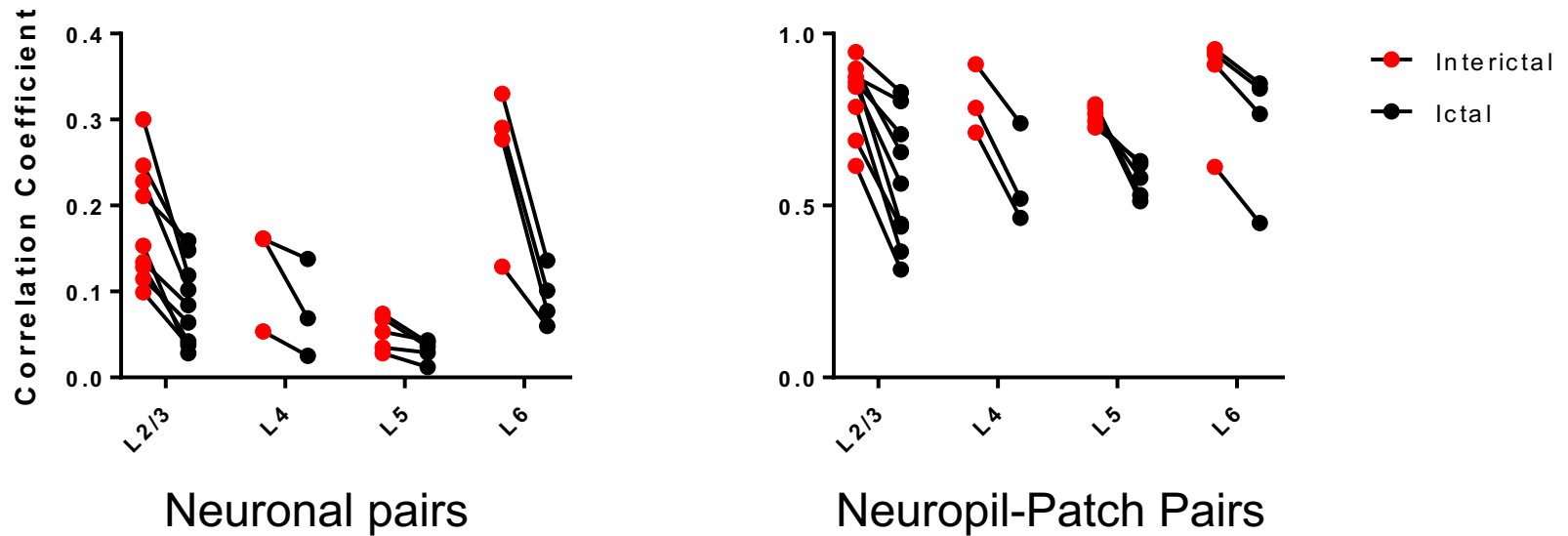
Example Data from one recording
(160 seizures)



Pooled data from all animals



Synchrony is reduced across layers



Each dot represents mean across one FOV

How do interneurons behave ?

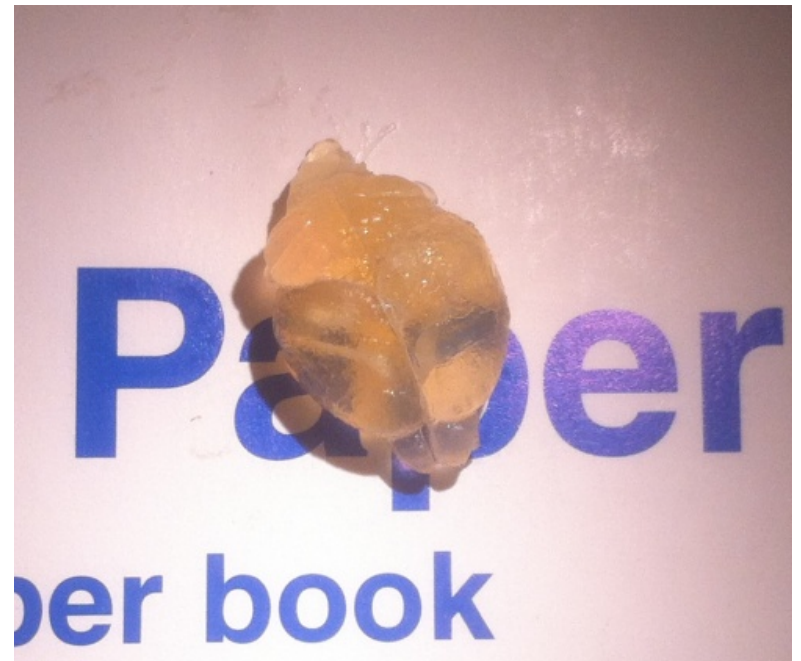
Identification of Interneurons

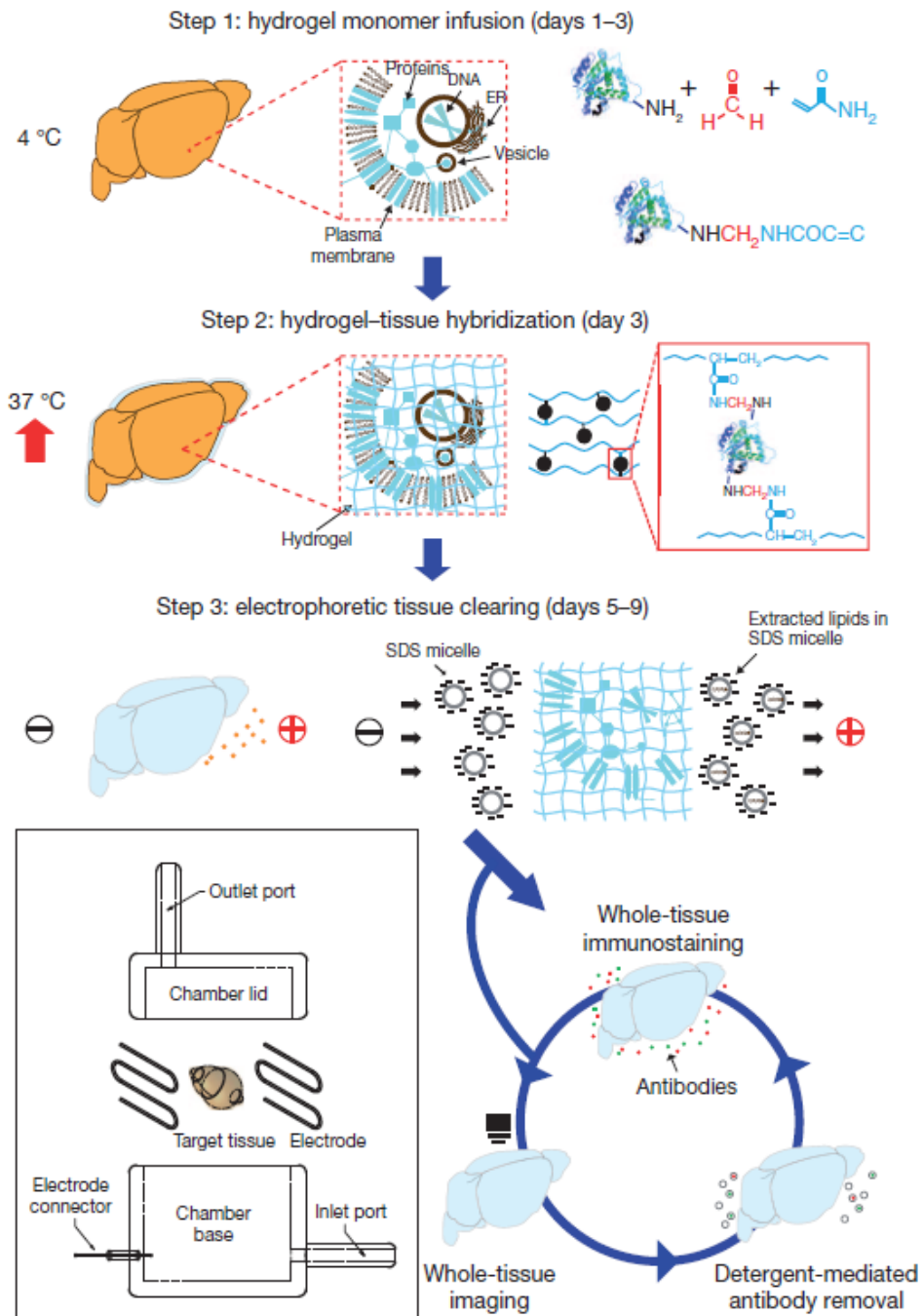
Structural and molecular interrogation of intact biological systems

Kwanghun Chung^{1,2}, Jenelle Wallace¹, Sung-Yon Kim¹, Sandhiya Kalyanasundaram², Aaron S. Andalman^{1,2}, Thomas J. Davidson^{1,2}, Julie J. Mirzabekov¹, Kelly A. Zalocusky^{1,2}, Joanna Mattis¹, Aleksandra K. Denisin¹, Sally Pak¹, Hannah Bernstein¹, Charu Ramakrishnan¹, Logan Grose¹, Viviana Gradinaru² & Karl Deisseroth^{1,2,3,4}

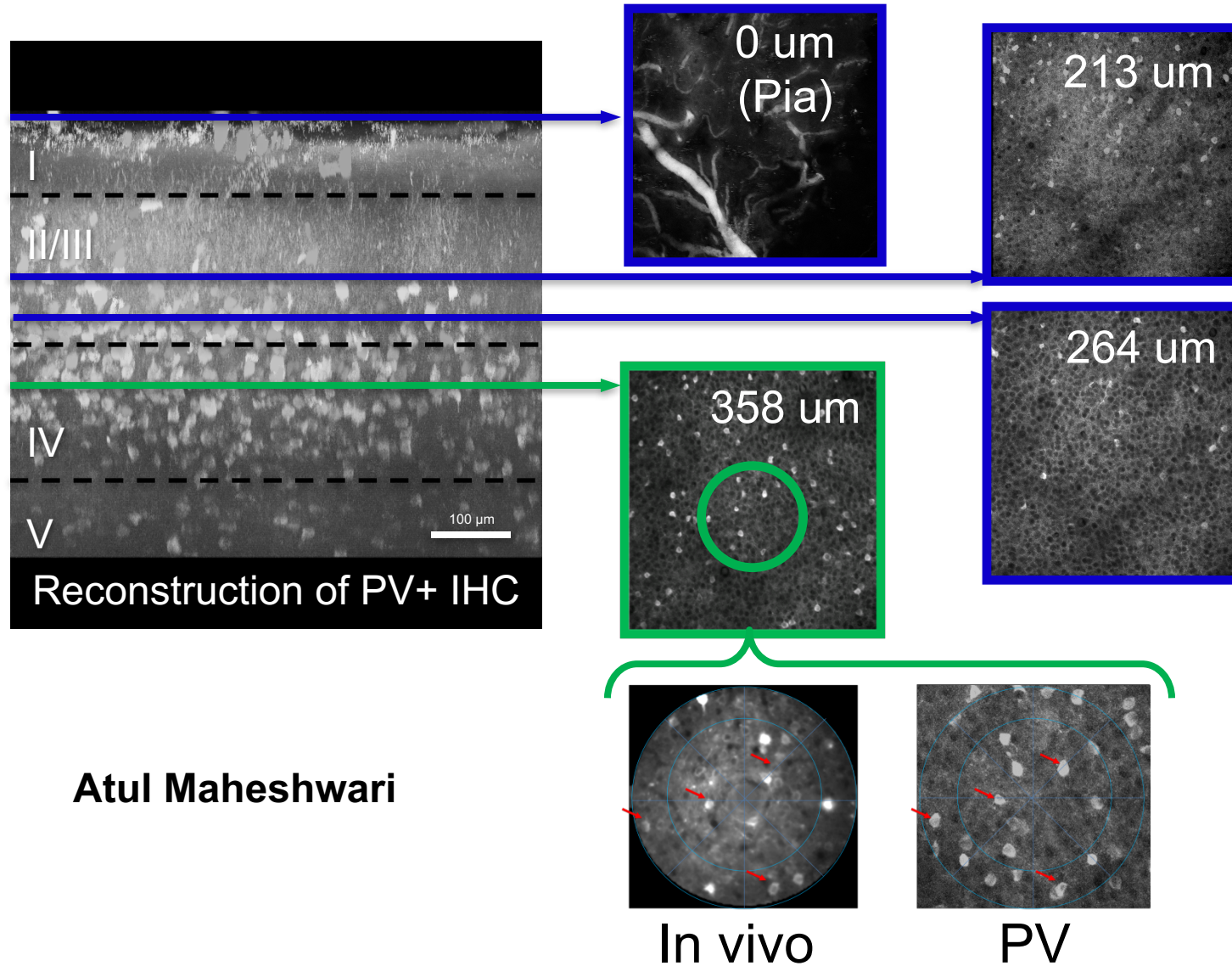
CLARITY:

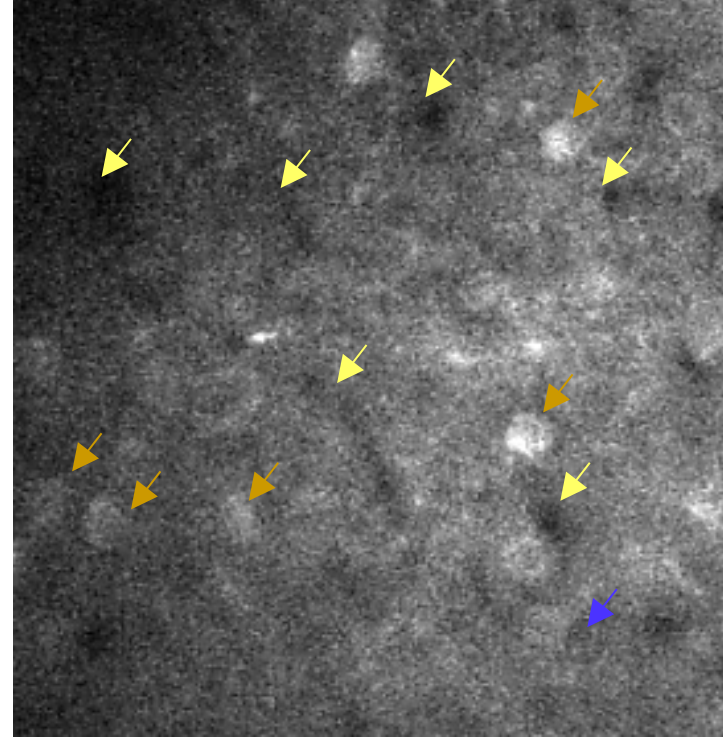
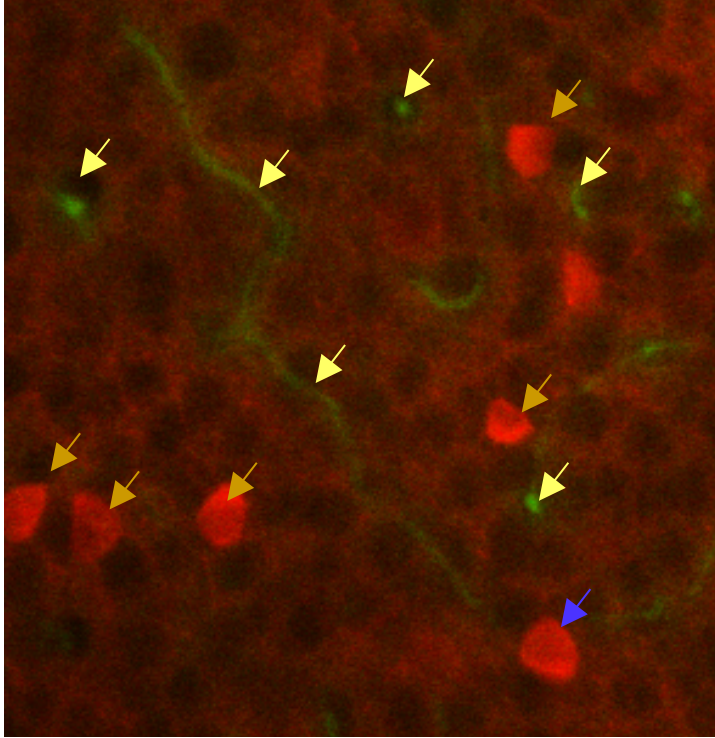
Clear **L**ipid-exchanged
Anatomically **R**igid
Imaging/immunostaining-
compatible **T**issue **h**ydrogel





Post-hoc CLARITY and immunostaining identifies PV+ interneurons





Atul Maheshwari

76 SST/PV Interneurons: **largely ictal low**

- Total number of interneurons (mix from all layers)
 - Dlx (SST/PV): 47 – 4 neutral, 43 ictal low
 - SST: 15 – 1 ictal high, 2 neutral, 12 ictal low
 - PV: 14 – all ictal low

Conclusions

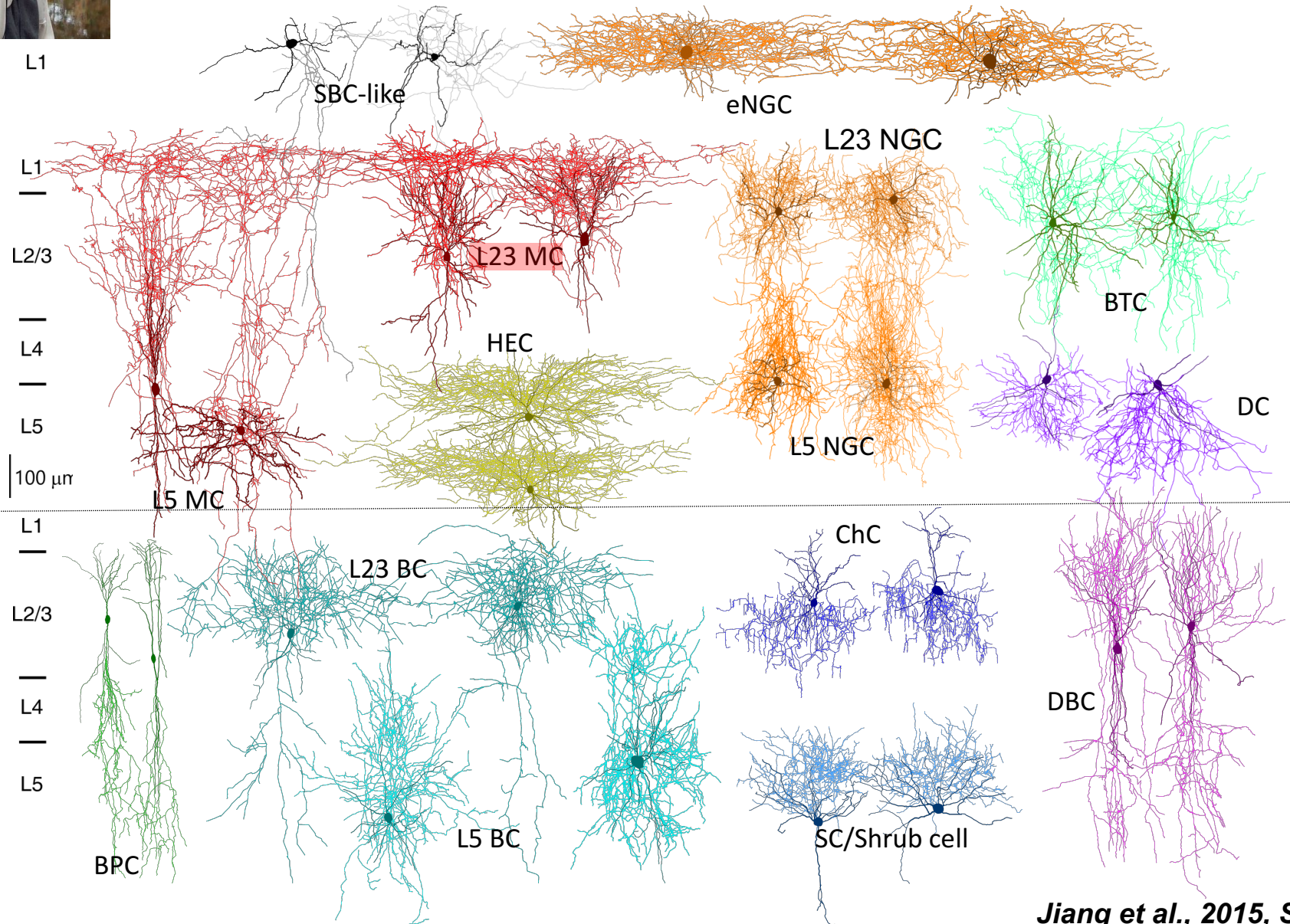
- Cortical activity is suppressed in stargazer mice area V1 during absence seizures. Both neurons and neuropil, behave similarly. SST/PV interneurons are also predominantly ictal low.
- The coupling of neurons to seizure activity is dynamic on time scales of minutes to hours, ictal lows are more stable than ictal highs, but neurons can change their character in long-term recordings.
- Surprisingly, pair-wise synchrony between pyramidal neurons is also lower during seizures (**caveat – we cannot exclude that a subgroup of neurons may intermittently synchronize at a much finer time–scale, but on average desynchronization seems to be the rule**).
- This is not due to increased interictal locomotion or generally higher firing rates between seizures.

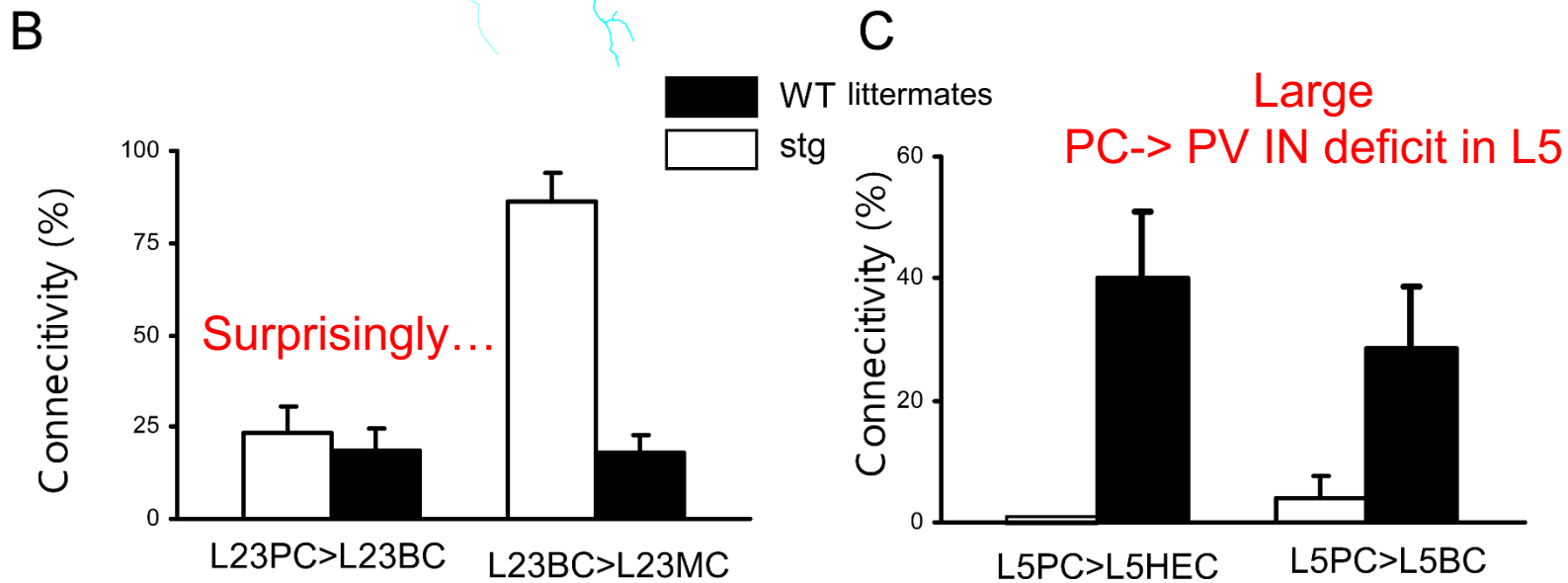
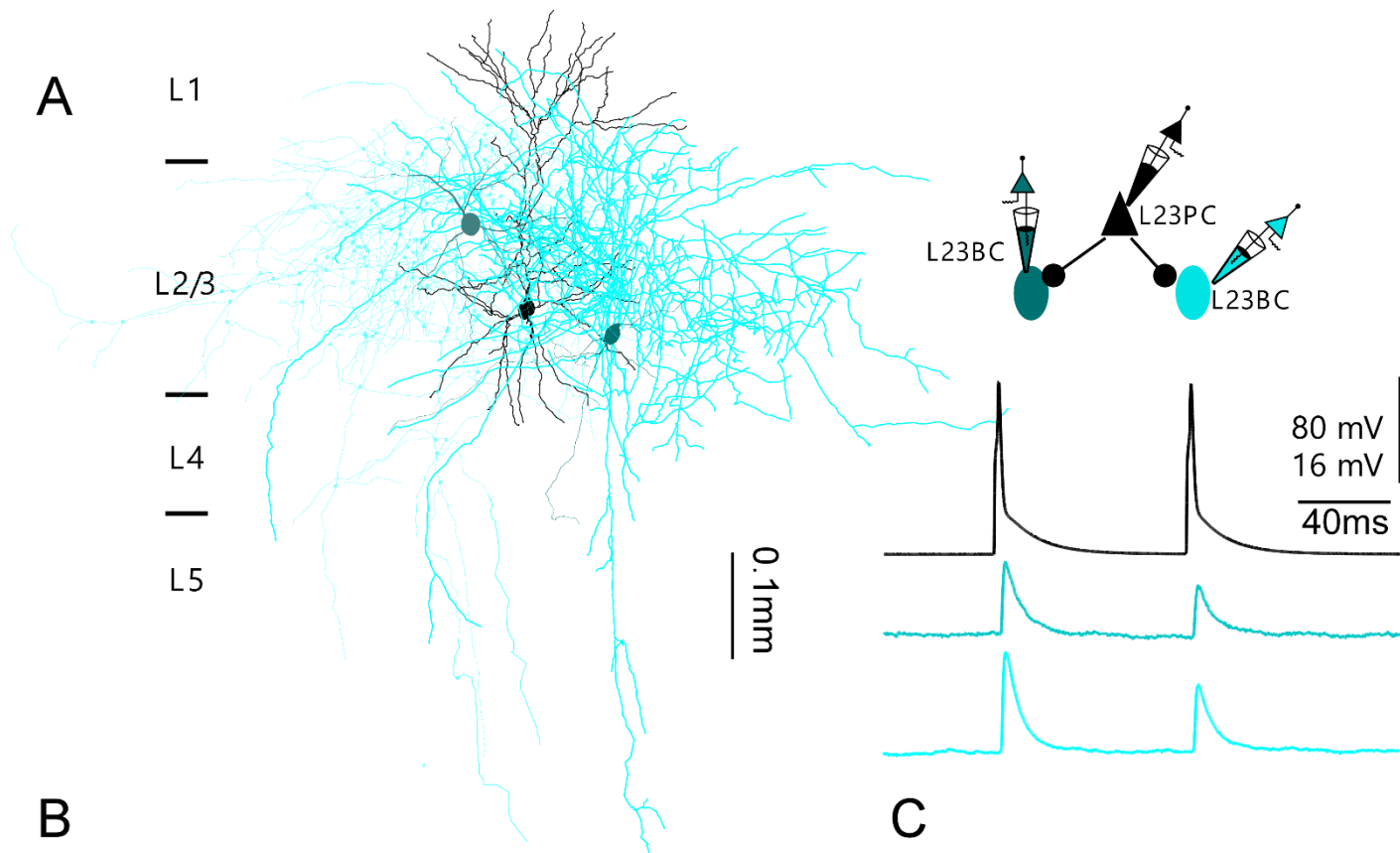
Can we start to understand the circuit pathophysiology?



Xiaolong Jiang, Baylor College of Medicine
Pre-eminent Patch Guru

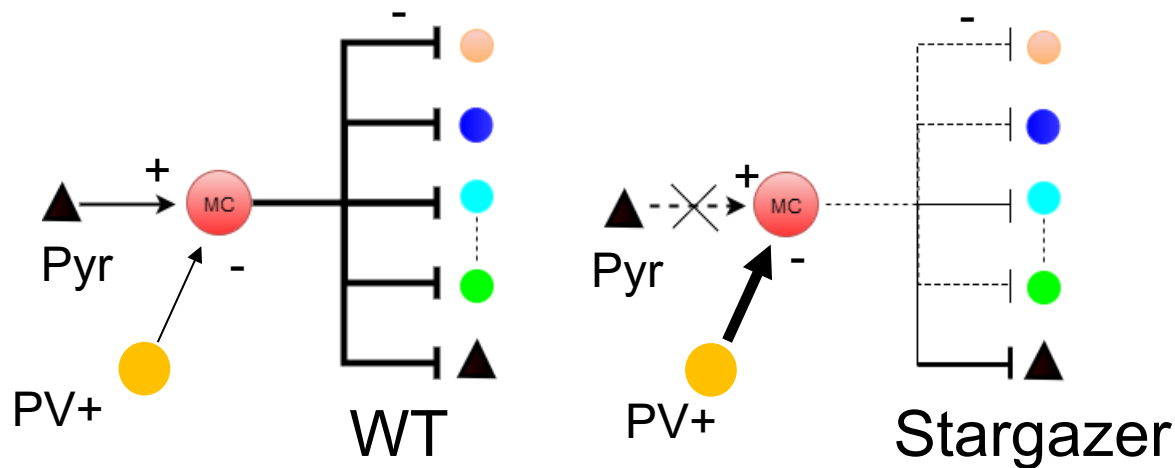
Morphology of 15 types of interneurons in L1, L2/3 and L5





Summary of (preliminary) circuit deficits in stg

- 1) L2/3Pyr → L2/3MC ↓↓↓
L2/3PV⁺ BC → L2/3MC ↑↑↑
L2/3 MC → interneurons ↓↓↓



- 2) L2/3Pyr → L2/3PV⁺ remain intact, but L5Pyr → L5 PV⁺ ↓↓

*"There are more things in heaven and Earth, Horatio,
than are dreamt of in your philosophy"*

CONCLUSIONS

- Cortical activity is suppressed and, on average, de-correlated in stargazer mice area V1 during absence seizures.
- The coupling of neurons to seizure activity is flexible from minutes to hours.
- Decreased PC to PV IN connectivity strength expectations from immunohistochemical analysis were supported physiologically in L5 but not L2/3
- Circuit analysis revealed multiple connectivity abnormalities, notably increased PV inhibition of L2/3 Martinotti cells, which fail to suppress other INs.
- We mostly observed ictal suppression in all cell types examined so far, suggesting this is driven by a master inhibitory regulator **or** the thalamus
- **An intensive, focused, interdisciplinary approach is required to dissect circuit function in well-defined epilepsy models, in order to fully understand circuit malfunction and identify appropriate circuit targets for therapy.**



HARVARD
MEDICAL SCHOOL

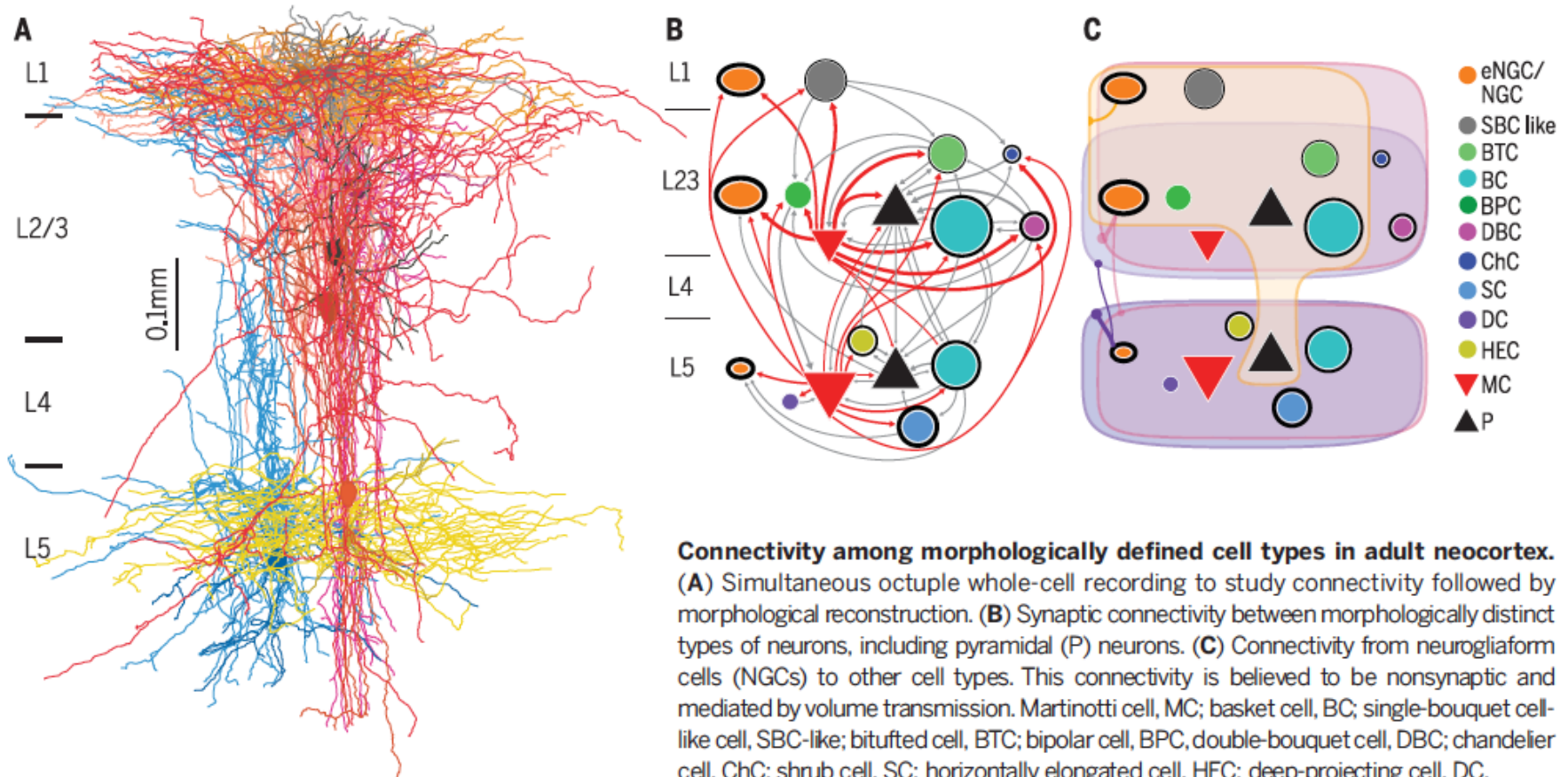
Baylor
College of
Medicine®

- Jochen Meyer
- Atul Maheshwari
- Xiaolong Jiang
- Jeff Noebels



- NINDS R21 NS088457, March of Dimes Award to SS
- T32 NS007399-08, Caroline Wiess Law Fund for Molecular Medicine, and K08 NS096029 to AM;
- NINDS NS29709 to JN

Anatomy of the Circuits is Complicated (but important principles can still be extracted)

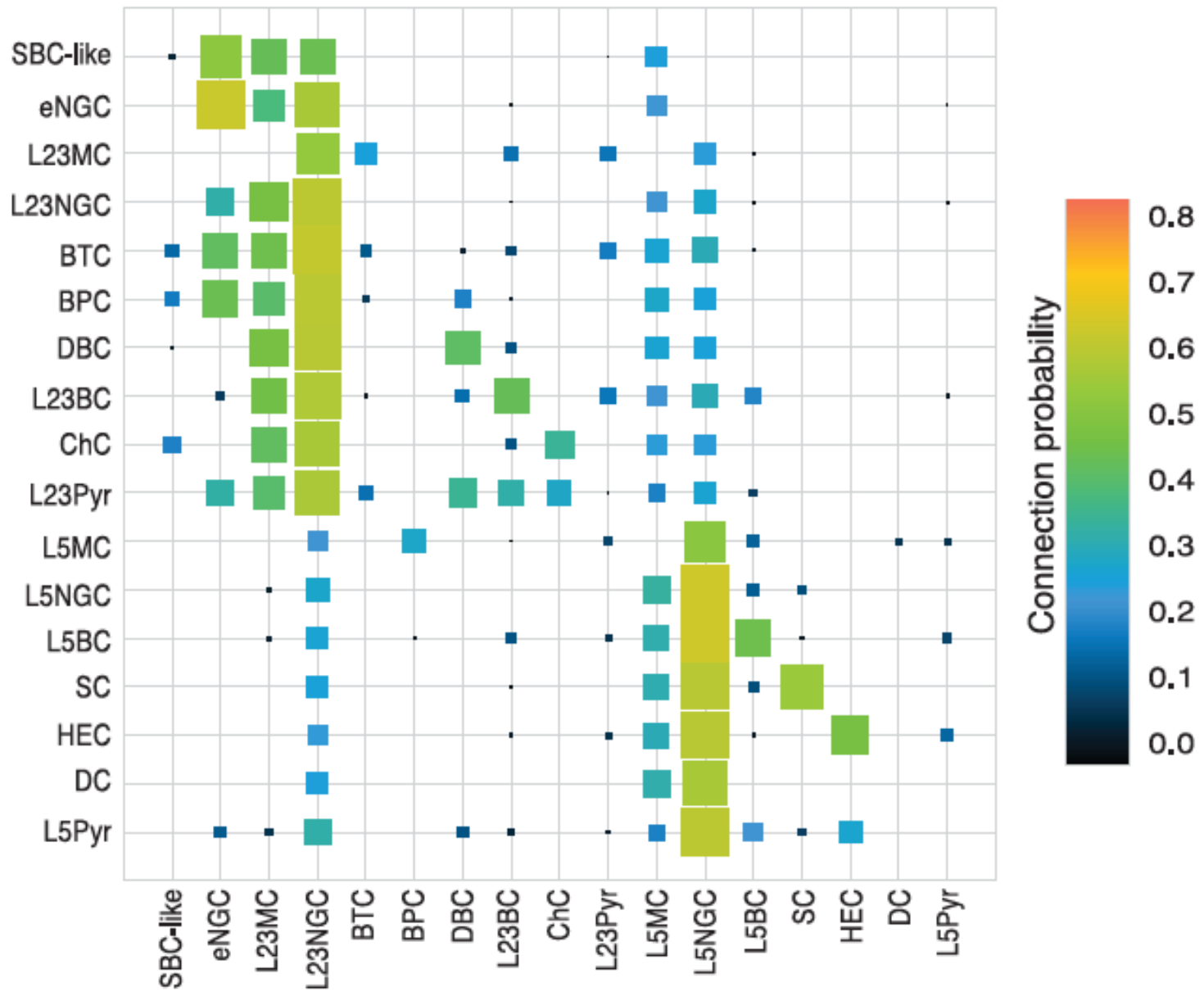


Connectivity among morphologically defined cell types in adult neocortex. (A) Simultaneous octuplet whole-cell recording to study connectivity followed by morphological reconstruction. (B) Synaptic connectivity between morphologically distinct types of neurons, including pyramidal (P) neurons. (C) Connectivity from neurogliaform cells (NGCs) to other cell types. This connectivity is believed to be nonsynaptic and mediated by volume transmission. Martinotti cell, MC; basket cell, BC; single-bouquet cell-like cell, SBC-like; bitufted cell, BTC; bipolar cell, BPC; double-bouquet cell, DBC; chandelier cell, ChC; shrub cell, SC; horizontally elongated cell, HEC; deep-projecting cell, DC.

Principles of connectivity among morphologically defined cell types in adult neocortex

presynaptic

postsynaptic



3 types of interneurons: 2 master regulators, Interneuron selective (not locally regulated and not self-inhibitory), Pyramidal specific (locally regulated, typically self-inhibitory)

Douglas and Martin – Mapping the ways of the neocortex (2008)

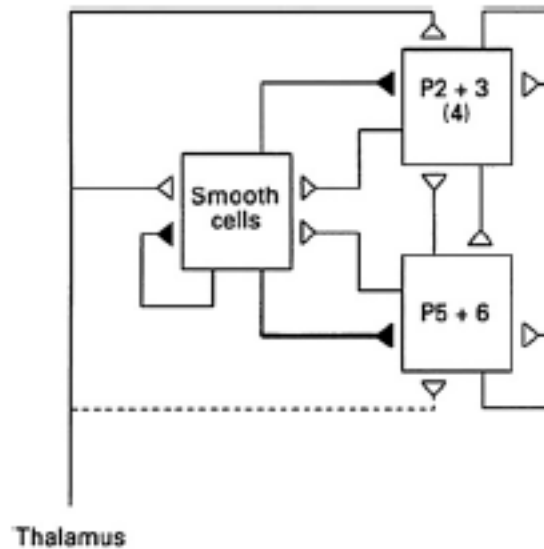


Figure 4. Canonical Cortical Circuit Based on Electrophysiological and Modeling Studies in the Cat Visual Cortex
From Douglas and Martin (1991).

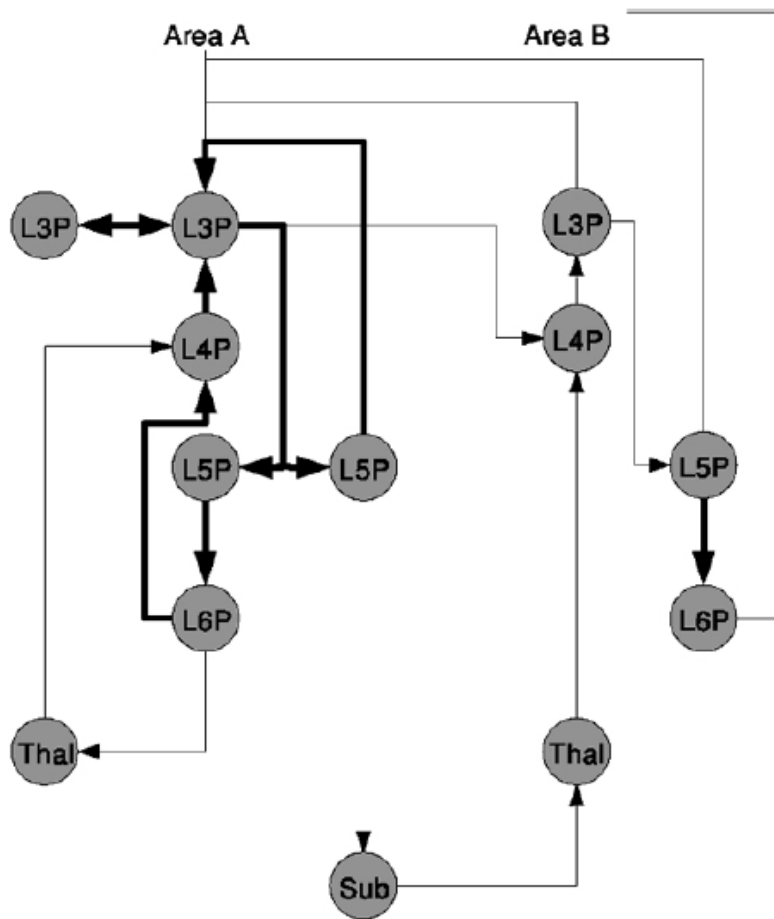


Figure 1 Graph of the dominant interactions between significant excitatory cell types in neocortex and their subcortical relations. The nodes of the graph are organized spatially; vertical corresponds to the layers of cortex and horizontal to its lateral extent. Directed edges (*arrows*) indicate the direction of excitatory action. Thick edges indicate the relations between excitatory neurons in a local patch of neocortex, which are essentially those described originally by Gilbert & Wiesel (Gilbert & Wiesel 1983, Gilbert 1983) for visual cortex. Thin edges indicate excitatory connections to and from subcortical structures and inter-areal connections. Each node is labeled for its cell type. For cortical cells, L_x refers to the layer in which its soma is located. P indicates that it is an excitatory neuron (generally of pyramidal morphology). *Thal* denotes the thalamus and *Sub* denotes other subcortical structures, such as the basal ganglia.

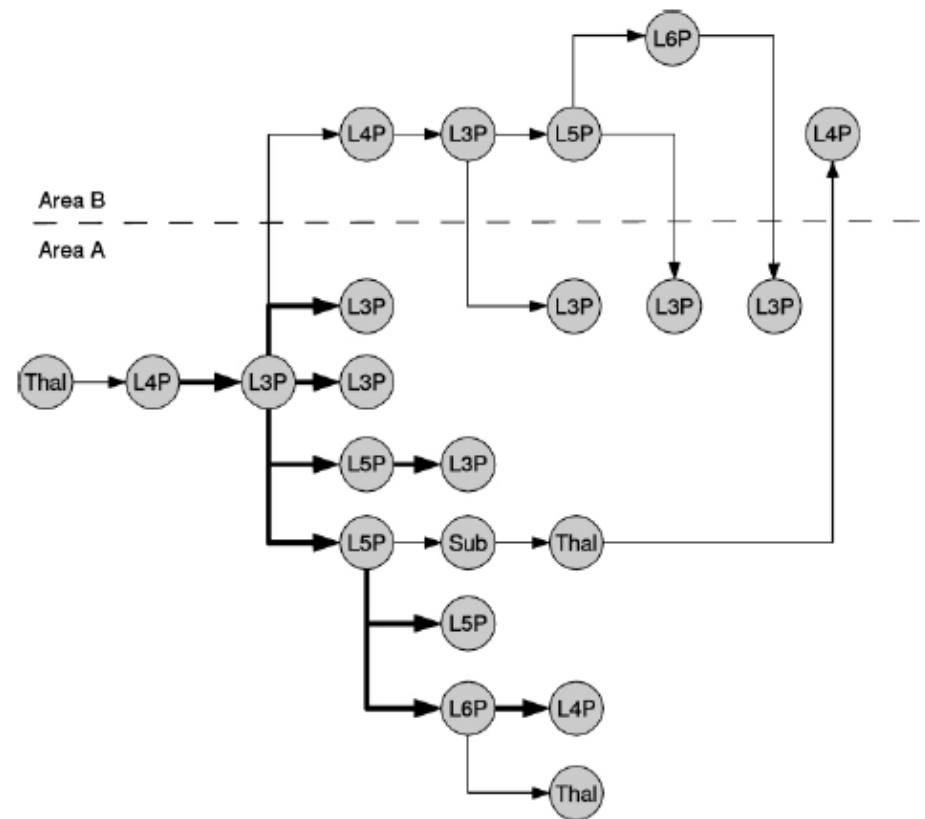


Figure 2 Graph of the temporal interactions between the cell types shown in Figure 1. Time unfolds toward the right. Each edge represents one synaptic delay. A temporal path ends when it is no longer unique; that is, further possible paths from that end node can be traced by selecting other nodes in the graph of the same cell type. For additional description, see Figure 1.

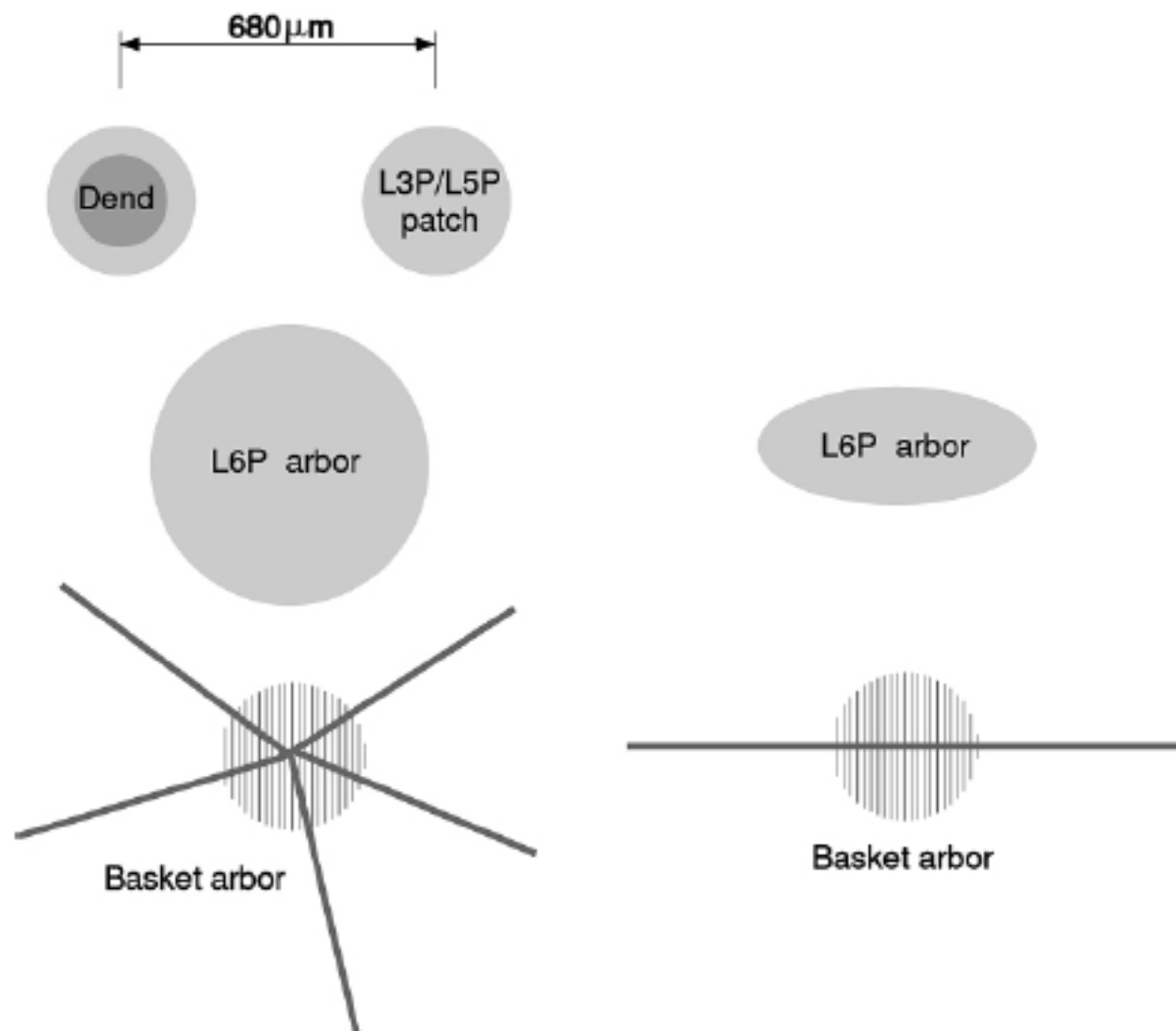


Figure 3 Approximate sizes of some important axonal arborizations, shown in tangential (*left*) and vertical (*right*) sections. Top: Diameter of layer 3 (or layer 5) patches (*light gray disk*, $320\ \mu\text{m}$ diameter), compared with that of the basal dendrites of a layer 3 pyramidal cell (*dark gray disk*, $200\ \mu\text{m}$ diameter). The inter-patch distance is $680\ \mu\text{m}$. Patch data were averaged

Computation Flow Between Groups of Neurons

Douglas Martin // Abeles
//Vaadia

[Temporal firing patterns of single units, pairs and triplets of units in the auditory cortex.](#)

Vaadia E, Abeles M.

Isr J Med Sci. 1987 Jan-Feb;23(1-2):75-83.

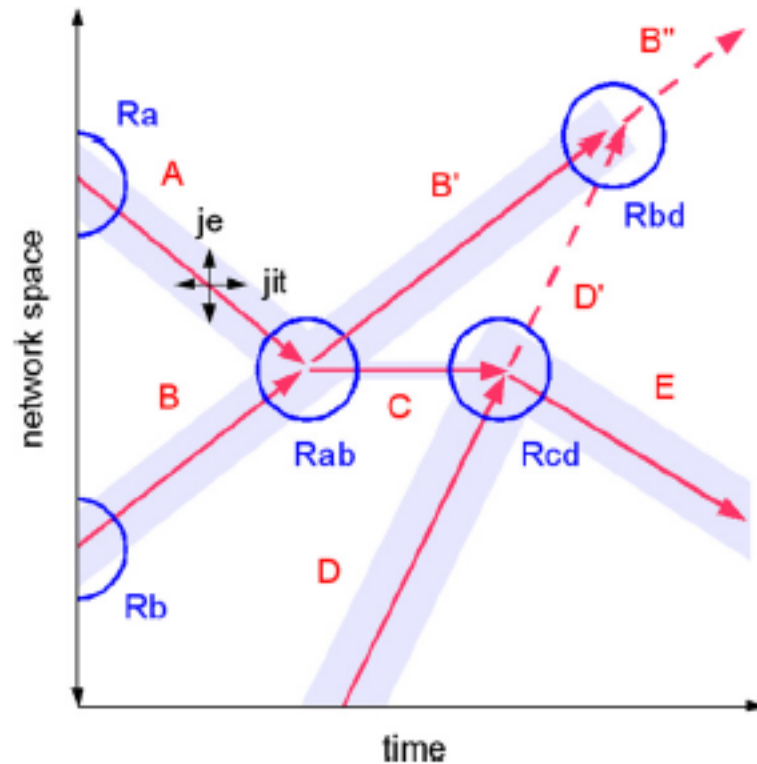


Figure 6. Schematic Representation of Just-Enough and Just-in-Time Computation in a Cortical Network

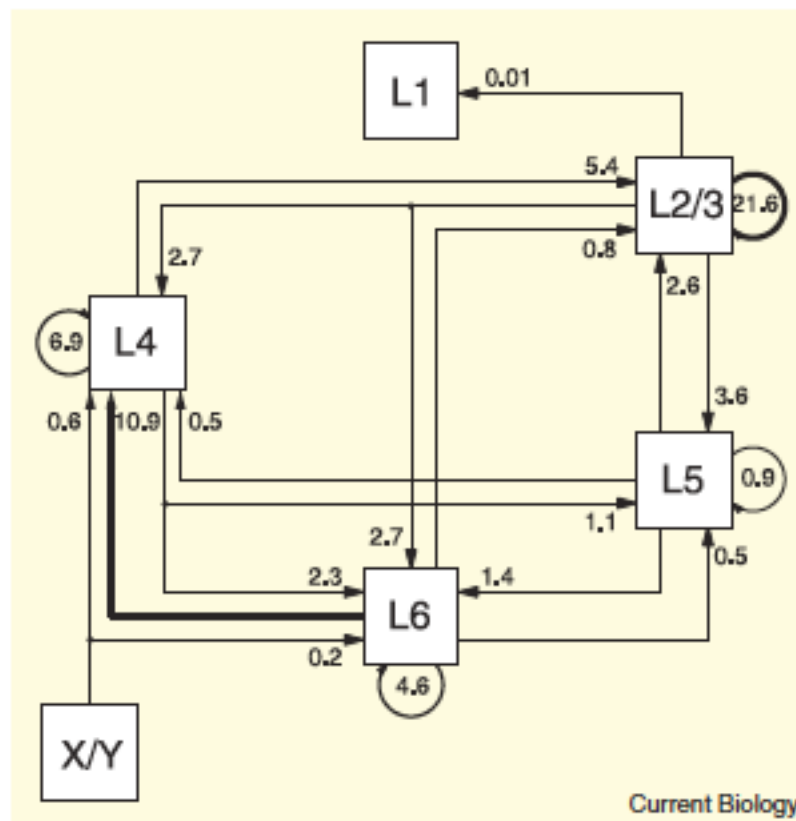
The computation is shown evolving in time in a network of neurons, represented here spatially in one dimension. Two local populations of neurons located at computational "rendezvous" nodes Ra and Rb emit messages composed of spatiotemporal spike patterns along the communication edges ("axons") indicated as red arrows. The "widths" of the connection pathways (the number of connections) and the temporal window during which they can be effective are indicated by the blue-gray paths flanking each arrowed edge (widths "je" and "jit"). Messages A and B are shown passing through a rendezvous node Rab. As a result of that local interaction, Rab emits messages B' and C. C in this case consists of a small number of neurons that hold their outputs steady for some interval until the arrival of message D at rendezvous node Rcd. The interaction of C and D then leads to the emission of message E from Rcd. As a result of this interaction, another possible output, D', from node Rcd does not occur, which means that a possible interaction between B' and D' in rendezvous node Rbd does not occur, and B'' is not emitted.

Recurrent neuronal circuits in the neocortex

**Rodney J. Douglas and
Kevan A.C. Martin**

Figure 1. A quantitative graph of the connections between various classes of excitatory neurons and their targets in cortex.

Only the connections between the classes of the dominant excitatory cell types are shown in this partial diagram. Each arrow is labeled with a number indicating the proportion of all the excitatory synapses in area 17 that are formed between the various classes of excitatory neurons. Total number of synapses between excitatory neurons is 13.6×10^{10} . Additional maps of connections from excitatory to inhibitory neurons, and so on, can be found in Binzegger *et al.* (2004).



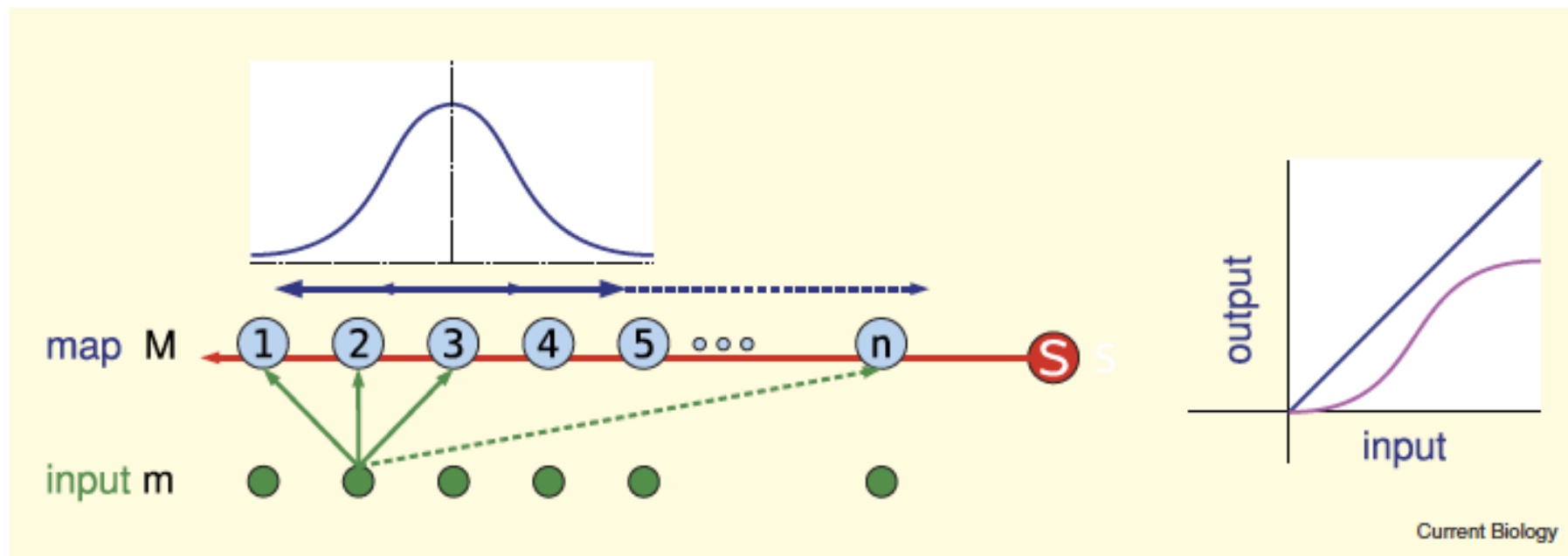
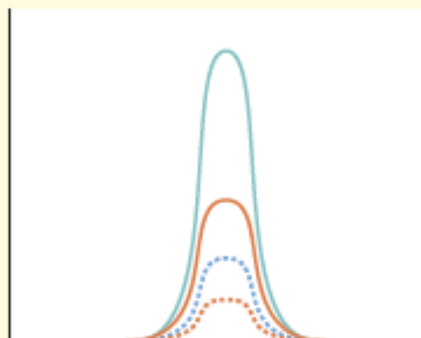


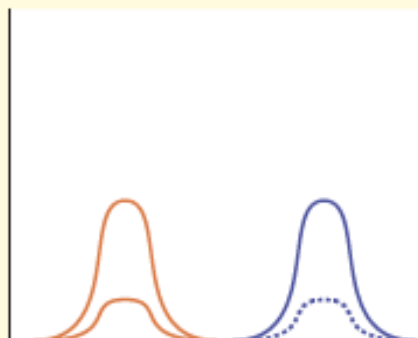
Figure 2. Simple model of recurrently connected neurons with rate coded outputs.

A population of N rate excitatory neurons (blue filled circles) arranged as a spatial array; each receives inhibition from a common inhibitory neuron (red filled circle), and each of them excites that inhibitory neuron. Each excitatory neuron receives feedforward excitatory input (green arrows from green input neurons), as well as recurrent excitatory input from their close neighbours. The strength of the recurrent inputs made onto any target neuron is a bell shaped function of the neighbour's displacement in the array from the target neuron (example shown for neuron 3). The activation function (right) of all neurons is a thresholded linear function (blue line) rather than a sigmoid (cyan). Unlike the sigmoid, the linear activation is unbounded above so that the stability of the network must depend on the integration of excitatory and inhibitory neurons rather than the sigmoidal saturation of individual neurons.

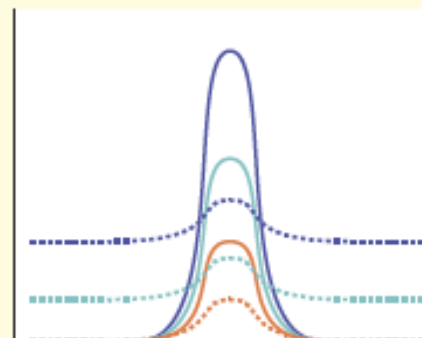
linear



linear analog gain
(above threshold)

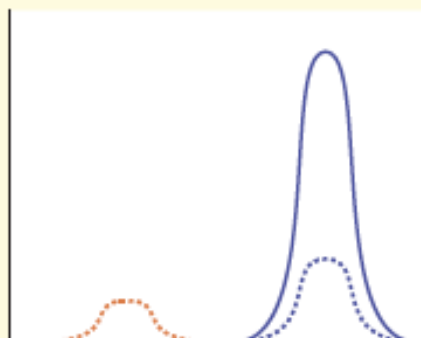


locus invariance

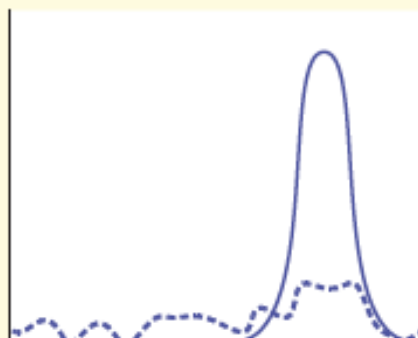


non-linear gain control
(by common mode input)

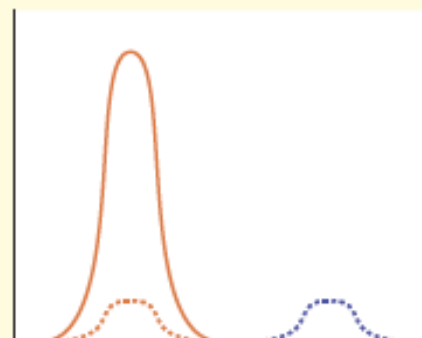
non-linear



non-linear selection
(<soft> winner-take-all)



signal restoration
(invariance)



multi-stability

Current Biology

Figure 3. Six interesting functional properties of the recurrent network described in Figure 2.

In this multi-part figure, each part shows the response of the array of excitatory neurons (along the x-axis). Top left: Linear Gain. Above threshold, the network amplifies its hill-shaped input (stippled lines) with constant gain (output, solid lines). Top center: Locus Invariance. This gain is locus invariant (provided that the connections' weights are homogenous across the array). Top right: Gain Modulation. The gain of the network can be modulated by an additional constant input applied to all the excitatory neurons, and superimposed on the hill-shaped input. The gain is least when no constant input is applied (input, red stippled line; output, red solid line), and largest for a large constant input (blue lines). Bottom left: Winner-take-all. When two inputs of different amplitude are applied to the network, it selects the stronger one. Bottom center: Signal Restoration. The network is able to restore the hill-shaped input, even when that input is embedded in noise. Bottom right: Bistability. When separate inputs have the same amplitudes, the network selects one, according to its initial conditions at the time the input is applied.

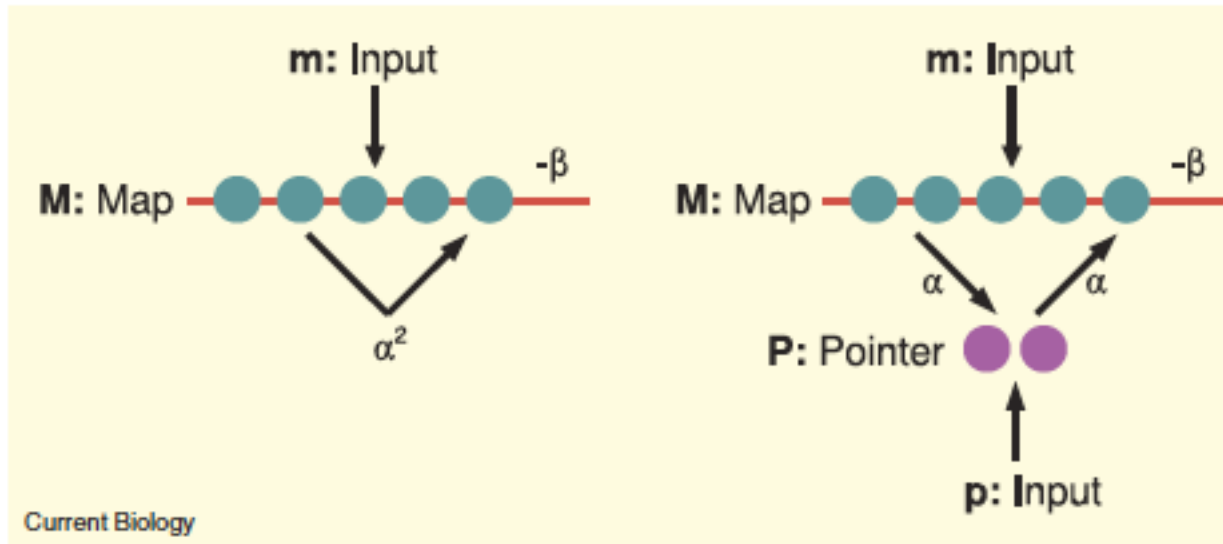


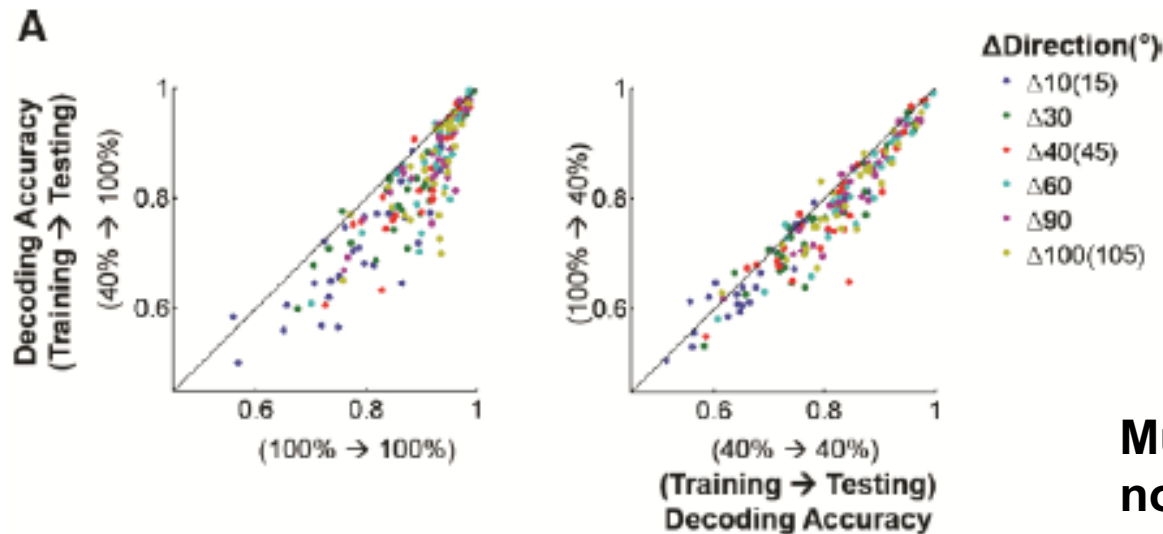
Figure 4. Comparison of standard recurrently connected network left (equivalent to Figure 2), and the 'pointer-map' configuration of recurrence.

Both networks have inhibitory feedback ($-\beta$, red). In both cases the overall feedback between excitatory neurons is the same. In the standard network this feedback is applied monosynaptically. In the pointer-map, a small, for example two cell, population of 'pointer neurons' is inserted in the feedback loop. In this way, the feedback is decomposed into two successive stages, each providing gain α . The two pointer neurons have differently biased connectivities to the map of excitatory neurons. The left pointer neuron is more strongly connected to the leftmost neurons of the map, and the right pointer to the rightmost neurons of the map. If the pointer neurons are not perturbed by their inputs (p) then the pointer-map behaves like the simple recurrent network at left. When the 'feedback' or 'top down' input p is applied, it differentially activates the pointer neurons, and so biases the distribution of feedback gain to the map. For example, if input p is applied only to the left pointer, amplification of 'bottom up' map input m will be increased towards the left of the map, and reduced toward the right, so providing an attentional focus toward the left.

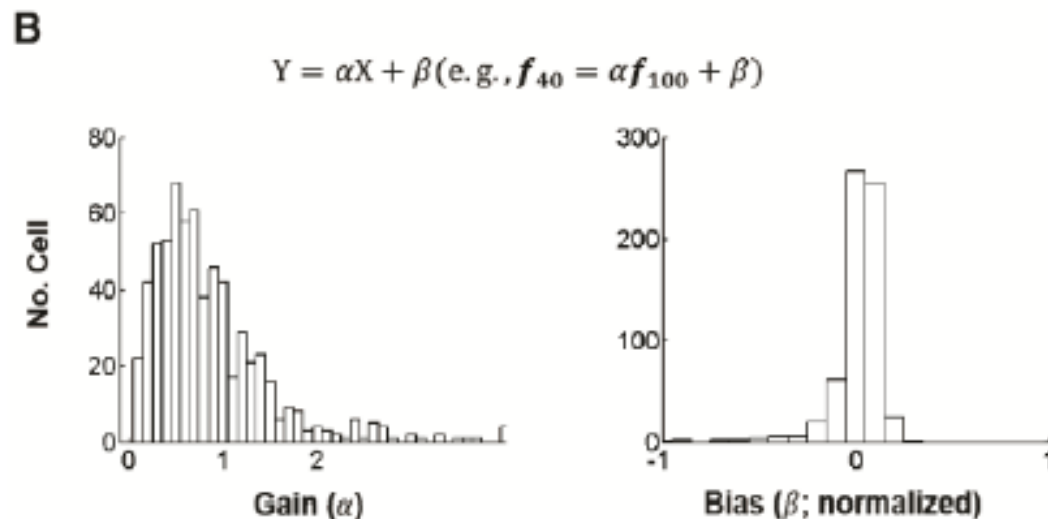
How does the code remain stable
wrt to internal fluctuations?

Stability of the Code on the Face of internal fluctuations

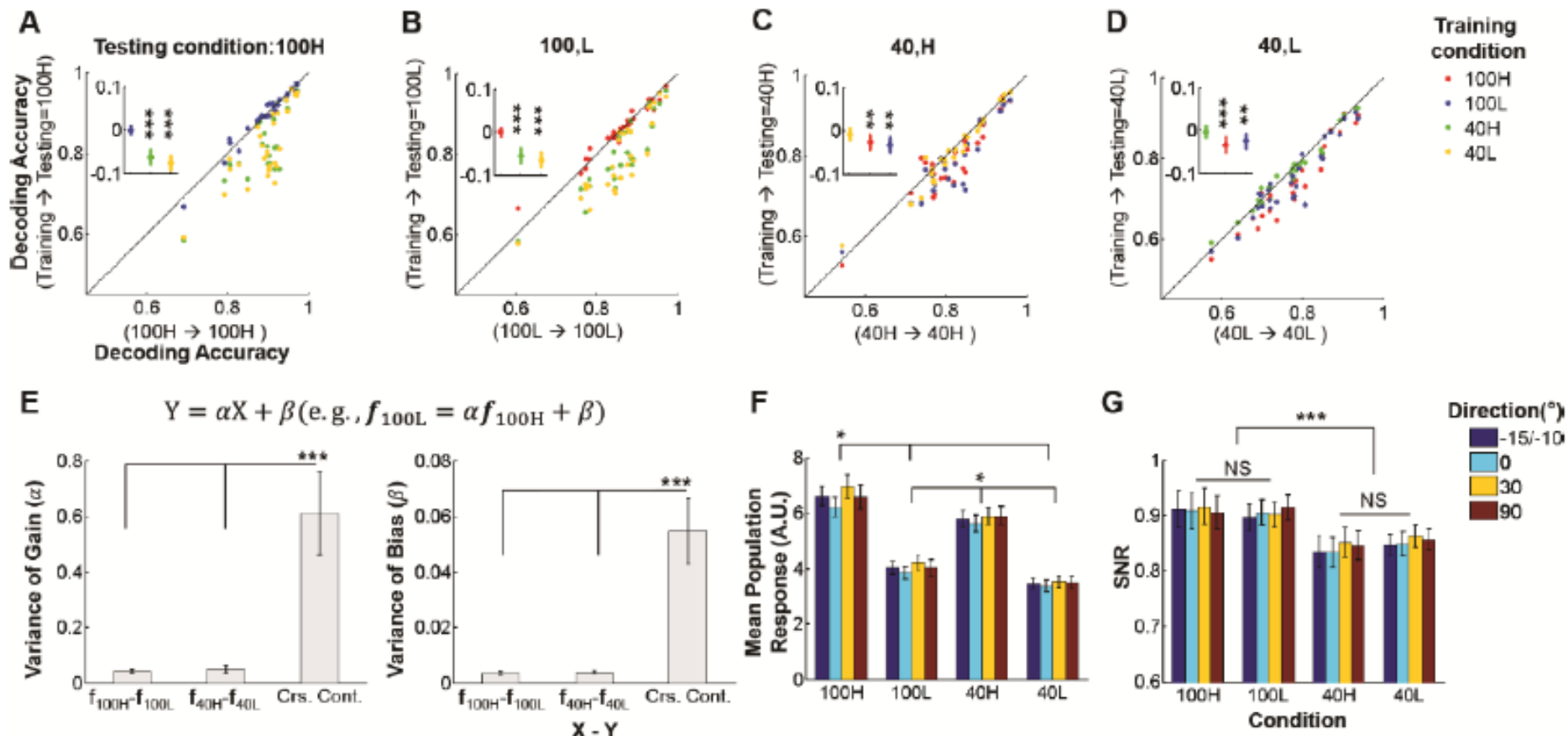
(Internal gain modulations, but not changes in stimulus contrast, preserve the neural code. S Lee, J Park, SM Smirnakis)

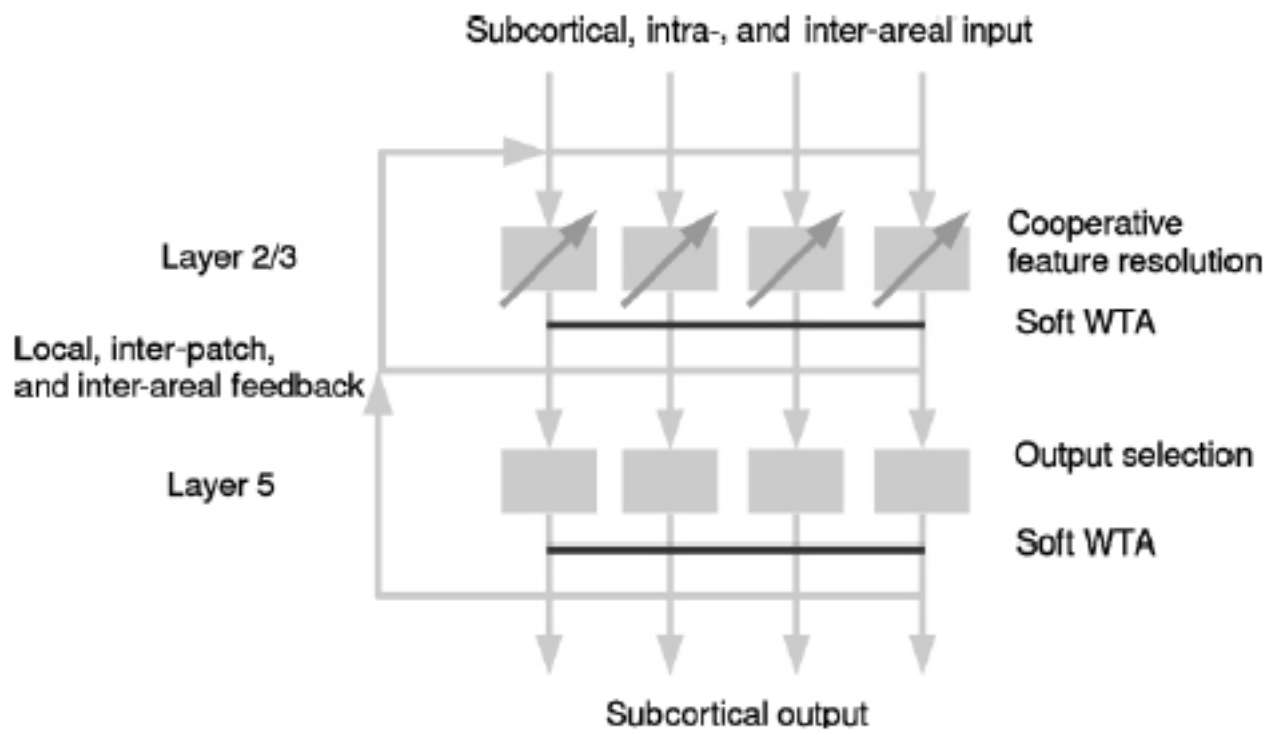


Multi-neuronal Code is not invariant wrt contrast



but it is invariant wrt internal state





Principles/Open questions

- Inherent ambiguity in neuronal firing – how does this get resolved – why does it occur in the first place?
- What are some of the properties that the representation of information on the cortical circuit should have?
- Canonical Computations? Normalization (Carandini – Heeger)?
- Internal Circuit Rhythms // State Dependent modulation of neural responses– How does the representation of information remain stable?
- Transformation of information representation --- projective to Euclidean geometry – advantages?
- When is representation stable and when is flexible? How does the computation remain stable on the face of flexible representations? How does information get transmitted through successive stages without apparent degradation in the brain (von Neumann)?
- Many inter-neuronal types – what type of control does each one exert? What is its impact on decoding or learning?
- How do networks behave during learning / forgetting?
- What network behavior allows complexity (or “creativity”) to emerge?